Anonymous Referee #1

Received and published: 8 May 2020 This paper presents the results from laboratory burning experiments of biomass fuels from east Africa. This is Part 2 of a companion paper. In this paper, the authors present the chemical characterization of the smoke sampled during the burns. Both fresh and aged smoke at 500oC (smoldering) and 800oC (flaming) is examined to explore the compounds that lead to the light absorbing properties of the smoke.

Overall, this is a good paper. It is not necessarily an easy read due to all the interpretation of mass spectra involved in the analysis. But I think the authors have generally done a good job in presenting it in a straightforward manner. I just have a handful of minor comments outlined below to help with the flow of the paper. These needs to be addressed before the paper can be considered for publication.

Authors response

The authors thank the reviewer for the positive comments and suggested revisions. The revisions done based on the comments are provided below each comment in italics.

Reviewers Specific Comments:

Line 22 – The authors mention Eucalyptus and Acacia as the fuels examined. Although they are the primary ones examined in this work, results from the burning of Olive are also presented. This should be noted in the abstract.

Line 183 – Suggest changing cases to case

We disagree with the reviewer, it's each case, not each cases. That doesn't sound right on the ear. "Each" is always singular.

Line 188 – Suggest adding after cases, respectively

Correct, this has been changed.

Line 245 – Suggest changing an m/z to a m/z

The original wording is correct, according to APA Style 6th edition. The acronym "m/z" is pronounced "em-zee", which starts with a vowel sound, and therefore is preceded by "an" instead of "a".

Table 1 – Believe that dimethoxybenzoic and nitrocresol should be one word

Correct, this has been changed.

Lines 330 and 339 – Believe that dihydroxyphthalic acid is misspelled

Correct, this has been changed.

Line 337 – Suggest changing an SSA to a SSA

The original wording is correct, according to APA Style 6th edition. The acronym "SSA" is pronounced "ess-ess-ay", which starts with a vowel sound, and therefore is preceded by "an" instead of "a".

Line 375 – Believe that hydroxybenzaldehyde and dimethyoxybenzoic acid should be one word
Correct, this has been changed.

Line 420 – Suggest changing indicated their molecular to indicating the molecular as well as listed them to listing them
Correct, this has been changed.

Line 443 - Believe that dihydroxyphthalic acid is misspelled
Correct, this has been changed.

Line 464 – Suggest adding an a before pyrolysis
Correct, this has been changed.

Line 465- Suggest changing to 290 nm to at 290 nm
Correct, this has been changed.

Line 483 – Believe that nitrocresol is one word
Correct, this has been changed.

Table 3 - Believe that dimethoxybenzoic and nitrocresol should be one word
Correct, this has been changed.

Line 510 – Suggest changing an SSA to a SSA
See above.

Line 520 – Suggest adding an a before greater
Correct, this has been changed.

Line 523 – Suggest adding the word region after mid-visible
Correct, this has been changed.

Line 526 – Suggest adding a the before uncertainty
Correct, this has been changed to "within the measurement uncertainty…".

Line 581 - Believe that nitrocresol is one word
Correct, this has been changed.

Line 588 – Suggest changing an SSA to a SSA
See above.

Line 604 - Believe that nitrocresol is one word
Correct, this has been changed.

Line 624 – Believe the phrase and analyzed the data should be removed as it is repeated in the next line

This has been corrected.

Line 698 – Believe that Prevot is missing accent marks
This name and others in this citation have had their accent marks added.

Line 713 – The journal title appears to be missing
This has been corrected.

Anonymous Referee #2
Received and published: 22 June 2020

While the topic of this manuscript is certainly within the scope of ACP, I have significant concerns regarding some of the experimental methods used and how these are presented. Furthermore, several key pieces of experimental data are not included, and many of the results are not clearly discussed and explained. I found it difficult to under- stand many aspects of the paper. The SI is a spreadsheet of data with several figures that are not discussed. Many of these are important figures that should be presented and discussed in the main paper to understand the experiments (such as the aerosol size distributions). I do not think this submission meets the standards in terms of quality or clarity required for ACP and that it would be challenging to revise the paper to meet the standards of ACP. Many of my serious concerns and questions below were raised in pre-review for ACPD and were not addressed by the authors. Therefore, I am concerned that they are not taking the peer review processes seriously and am also significantly concerned with the reliability of many of their results. I conclude that it will be very challenging to substantially revise this manuscript to meet the standards of ACP and must recommend it be rejected.

Authors response
We do appreciate the concern of the reviewer and we would like the reviewer to know that we do take the review process very seriously and we will address all the concerns. The closing of labs due to COVID 19 and the relocation of the experimentalist who ran the chemical characterization experiments to Europe made it difficult to address all concerns in a timely manner earlier. However, the concern about the reliability of our results is somewhat biased and unfounded and insulting and we reject that concern. Our labs both at NCAT and UNC-Chapel Hill have maintained the highest ethical standards in our work and we stand by our results.

Most of the details of the experimental methods related to generation of biomass burning aerosols, burning conditions, details of the smog chamber used and the measurement of the optical properties is already described in Part I of this work (Smith et. al. 2020), and referenced in this paper. We have however provided enough and appropriated details in this paper. In response to the reviewer's concern we will have a separate supplemental document of figures that were placed in the spreadsheet. The discussion in the manuscript will refer to these figures in the revised manuscript. Additional figures and more details of the analysis will be provided in the revised manuscript to address all the concerns.

Reviewer Comment
The central issue is the experimental design seems poor. Very high aerosol mass concentrations are added to the chamber, and even after 12 hours of aging these only increase by half. This is a lot of time for semi-volatiles to partition to the walls which will cause additional "aging" that does not really simulate atmospheric aging processes; you will lose a lot of the semivolatile compounds that are strongly involved in atmospheric photooxidaton processes. There is a wide body of information on this specific to the dynamics of BBA and the key roles of dilution and evaporation such as from the FLAME experiments. It is also not clear how much aerosol is left in the chamber after 12 hours of aging, and the aerosol size distributions are not shown in the main paper. In the size distributions in the SI it appears there is substantial aerosol growth, but this is also not discussed. The high aerosol chamber mass concentrations will result in a lot of semi-volatiles being partitioned to the aerosol phase which will affect how they respond to photochemical aging since this occurs quite differently in the gas phase versus in the aerosol phase.

Authors response
The authors are bound by the limitations of their (or anybody's) instrumentation. Insufficient particle concentrations, particularly after aging, would preclude any meaningful measurements. In addition, had the authors used smaller concentrations, the wall loss of semivolatiles would become more important. Therefore, researchers that study SOA formation, for instance, frequently use ammonium sulfate seed particles, but such seeding was neither necessary nor desirable in this work.

Reviewer Comment
A relationship between BrC components and volatility has been found and would play an important role here though this is never discussed here. See for example the recent work of Rawad Saleh. Many studies on chamber aging and the role of dilution and evaporation of BBA have been reported and need to be discussed and used to interpret these results. See the many papers from the 4 prior FLAME campaigns, such as the work of Andrew May and Allen Robinson, and the more recent papers from the FIREX lab studies. The chamber studies of BBA aging reported by Ahern et al. from FLAME-4 are especially relevant to this work. Jeff Pierce has also examined the key interplay between fire size, dilution, and the resulting gain or loss of OA with "aging".

Authors response

We agree with the reviewer that dilution driven evaporation of BBA could potentially impact some aspect of our result. However, we don't think that will have a major impact on our conclusion. We believe these issues are critical for the organic aerosol enhancement studies like Ahren et al. and many more FLAME and FIREX studies as mentioned by the reviewer. Furthermore, we agree with the reviewer that some of the highly volatile BrC could potentially evaporate during this dilution process but as shown in a recent paper by Hodshire et al. (2019), our case would have low dilution driven evaporation due to a relatively larger load of OA.

Reviewer Comment
ppm levels of a few VOCs also appear to be added to the chamber during the UV aging but the purpose of this is not explained. Thus, the aging consists of high mass concentrations with high amounts of a few VOCs added but no additional oxidants added, and UV photochemistry. What

type of realistic atmospheric aging does this represent? The high aerosol mass concentrations represent in-plume concentrations while in the atmosphere most photochemical aging will occur under much more dilute conditions as the smoke entrains background air, and possible additional oxidants. Adding such high concentrations of VOCs is also odd as this would not occur as the smoke plume (a large source of VOCs itself) spreads and dilutes. Without a better handle on what specific type of aging is simulated here and how it represents atmospheric processes it is difficult to extrapolate these experiments to understand the real atmosphere. The focus is on understanding the sources, properties, and evolution of brown carbon.

Authors response

Some of the details of VOC addition is discussed in the first part of this paper (Smith, 2020). The purpose of adding the VOCs was to represent a polluted urban environment, where we used the emission inventory for urban environments from South Africa. This does not necessarily represent the east African emission inventory, but this serves as a baseline, since this is the only available data to us for the continent.

The concentration injected into the chamber was approximately 7 – 26 times more concentrated than values found from urban South African emissions and 6 – 18 times more concentrated than suburban values. The reason for these elevated levels was mostly due to sample preparation constraints, since the amounts needed for an exact match were too small for our scale to weigh appropriately. It is also plausible that the concentrations in east African emerging megacities can be that high since there are no regulations and many VOC sources. Concentrations in the chamber were intentionally higher than atmospheric conditions, to age the BB aerosol faster and accentuate the potential effect of SOA. No additional oxidants were added. This does not necessarily represent a realistic atmospheric aging environment but provides an insight for proper realistic experimental design. A limited number of fuel-specific comparisons can be made between the laboratory and field studies (Hodshire, 2019). Unlike field campaigns, laboratory campaigns keep chambers at an effectively fixed dilution ratio, so direct comparisons are not possible,

Despite the use of anthropogenic VOCs at concentrations larger than those average values found in urban and suburban regions of South Africa, no distinct effect was observed for SSA values of BBA produced during combustion at 500 °C. While it is possible that the relatively long aging time could obscure some of the effects due to the presence of VOCs, it is also possible that combustion products dominate molecular species and the effects of additional VOCs are insignificant. The latter would suggest that these added VOCs to represent urban pollution did not seem to affect the optical properties of BBA. A higher temporal resolution is needed to simulate the impact of the VOCs on aerosol SSA, where continuous or much more frequent measurements are needed. Since we size select particles in our work continuous measurements cannot be performed with our setup.

Changes made in the Manuscript:

The following is added in section 2.

"Details of VOC addition is discussed in the first part of this paper (Smith, 2020). The purpose of adding the VOCs was to represent a polluted urban environment, where we used the emission inventory for urban environments from South Africa. This does not necessarily represent the east

African emission inventory, but this serves as a baseline, since this is the only available data to us for the continent.

Reviewer Comment
Nitration of organics such as aromatics is known to play a prominent role in BrC production yet the role of nitrogen oxide chemistry is not discussed. 12 hours of photochemistry will likely deplete most of the NOx/NOy while this would not necessarily be the case under atmospheric conditions.

Authors response
It is unfortunate that NOx measurements were unavailable during these experiments, as the authors wish they could better address the primary emissions of NOx and its abundance over time as the sample ages. We address the role of nitrogen oxide chemistry in a discussion of catechol, along with other nitro aromatics, in a reviewer response below.

Reviewer Comment
Allowing the biomass fuel to dry in a hood for a year will drive evaporative loss of a substantial fraction of the organic components that can be emitted or are combusted in biomass burning, thus substantially altering the composition of the BBA measured here compared to realistic biomass burning. This aspect needs to be discussed as it can significantly alter the composition of the resulting BBOA and SOA. See Ahern et al. for a discussion of this:

Ahern, A. T.; Robinson, E. S.; Tkacik, D. S.; Saleh, R.; Hatch,L. E.; Barsanti, K. C.; Stockwell, C. E.; Yokelson, R. J.; Presto, A. A.; Robinson, A. L.; et al. Production of Secondary Organic Aerosol During Aging of Biomass Burning Smoke From Fresh Fuels and Its Relationship to VOC Precursors. J. Geophys. Res. Atmos. 2019, 124 (6), 3583–3606.

Authors response
We agree with the reviewer that long term drying of fuels will drive evaporative loss of organic compounds. This is also true for most domestic use of biomass fuels in the region where this study is focused on. Dried eucalyptus and acacia biomass fuels are common domestic fuels in east Africa. The moisture content of the samples was 10%. The reviewer's comment is valid if we try to make comparisons with wildfires, but fresh, wet fuels would not be used for domestic heating and cooking. Additionally, there are transportation problems (i.e. rotting) when dealing with fresh wood samples. The method used here actually preserves semivolatiles better than other potential drying methods, such as drying in the sun or in an oven. This is because the yield of essential oil upon distillation of Artemisia nilagirica (clarke) pamp leaves (another species whose oil contains significant quantities of eucalyptol) was largest for shade-dried samples (Anjum, et al. 2015).

Reviewer Comment
UPLC is used to separate the methanol extract of the BBA filter samples, but no chromatograms are shown. This is critical as BBA is notoriously difficult to separate using a C18 or similar reverse-phase column, and these chromatograms are used here in much of the analysis.

Authors Response:

Chromatograms of m/z vs. retention time (RT) vs. abundance of ions from UPLC/DAD-ESI-HR-QTOFMS for all the experiments were shown in SI. Although it can be challenging to separate BBOA constituents using a C_{18} reverse-phase column with UPLC (Di Lorenzo et al., 2016), our UPLC method clearly resolved most of the most methanol-extracted BBOA constituents from RT=5 to 14 min using a C_{18} reverse-phase column. However, we acknowledge that our UPLC/DAD-ESI-HR-QTOFMS method has the following limitations: We only used ESI operated in the negative ion mode (which doesn't ionize all BrC components - mostly the acidic ones), we used only RPLC (which may not resolve the high-MW BrC components, like SEC columns do as shown in Cora Young's work, due to poor separation or permanent retention on the RPLC column). However, we are likely to detect freshly produced smaller MW species with our method that ionize in the negative ion mode. Please see below for more details.

– To demonstrate the utility of our method to detect and resolve some of the BrC components we have added new figures, such as Figure 6.

Chromatograms of UV/Visible absorption vs wavelength and retention time for each fuel, age, and burning condition have been included in the SI and are referenced within the paper. Here is one example, from freshly combusted Acacia at 500 °C:

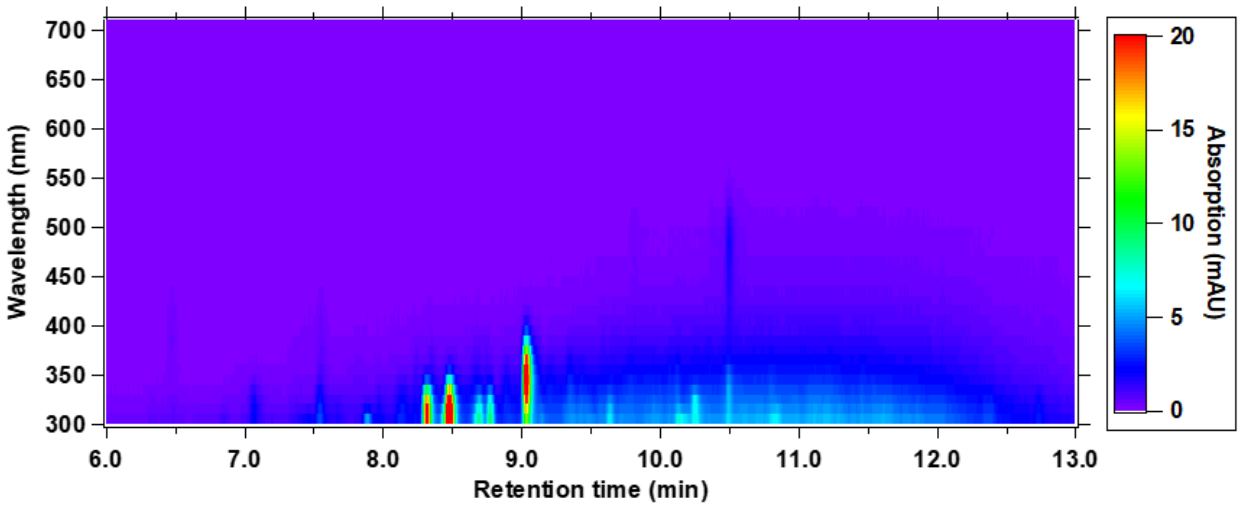

Reviewer Comment

Cora Young has a series of papers, on the use of size exclusion chromatography that discusses issues in UPLC analysis of BBA that should be consulted and discussed, as well as what they have learned regarding the relationship between BrC and molecular weight. Showing the chromatograms, at least in the SI, is also important as there are some weird baseline correction issues mentioned in the paper. Throughout the paper the properties of BrC obtained from other studies, not on these same systems are extrapolated to also describe the BrC/OA in these experiments. This is not a safe assumption.

Di Lorenzo, R. A.; Place, B. K.; VandenBoer, T. C.; Young, C. J. Composition of Size- Resolved Aged Boreal Fire Aerosols: Brown Carbon, Biomass Burning Tracers, and Reduced Nitrogen. ACS Earth Sp. Chem. 2018, 2 (3).

Di Lorenzo, R. A.; Washenfelder, R. A.; Attwood, A. R.; Guo, H.; Xu, L.; Ng, N. L.; Weber, R. J.; Baumann, K.; Edgerton, E.; Young, C. J. Molecular-Size-Separated Brown Carbon Absorption for Biomass-Burning Aerosol at Multiple Field Sites. Environ. Sci. Technol. 2017, 51 (6).

Di Lorenzo, R. A.; Young, C. J. Size Separation Method for Absorption Characterization in Brown Carbon: Application to an Aged Biomass Burning Sample. Geophys. Res. Lett. 2016, 43 (1), 458–465.

Authors response

As shown below in the responses, the BrC constituents are detected by RPLC since we interfaced it to the DAD and ESI-HR-QTOFMS detectors, assuming they ionize in the negative ion mode. We acknowledge that some of these light-absorbing compounds shown in Figure 6 may not ionize in the negative ESI mode. However, the elemental composition determined from the accurate mass measurements tells us something about the molecular composition, and thus, the double bond equivalents(DBEs). Prior work, such as in Lin et al. (2014, ES&T) showed that RPLC interfaced to DAD and ESI-HR-QTOFMS could resolve BrC components that eluted at the same retention times in the DAD and the ESI-HR-QTOFMS chromatograms; specifically, the structures chemically characterized by the ESI-HR-QTOFMS had the highest DBEs and likely explained the light-absorbing properties from IEPOX-derived SOA. In addition, this same method has been applied to urban aerosols (Zhang et al., 2013, ES&T) and BBAs derived from the combustion of Indonesian biomass (Budisulistiorini et al., 2017, ES&T). Notably, BrC components derived from Indonesian biomass was only characterized in the negative ion mode in the Budisulistiorini et al. (2017, ES&T) study. In addition to these studies, there is a lot of literature showing that as the organic component increases in DBEs the more likely it will absorb light. However, if the retention time in the ESI-HR-QTOFMS doesn't provide a formula that supports it would absorb in the BrC region (as measured by the DAD), then it is likely we missed it due to ESI operated in the negative ion mode. Other studies (including some of our own work with IEPOX SOA) have also used ESI in the positive ion mode since some BrC components preferentially ionize in that ion mode of ESI. However, even ESI can be blind to some BrC features seen in DAD, as explained by several papers from Prof. Alex Laskin's group. Prof. Laskin's group has shown that APPI is another ionization source that might help to better determine some of the BrC features seen in LC/DAD data.

The RPLC/DAD are powerful and show the light-absorbing aerosol components, but we must be careful in assuming that ESI operated in negative ion mode characterizes all of these. ESI operated in negative ion mode is very good at measuring acidic species, especially things like nitro-aromatics (e.g., nitrocatechols) (Zhang et al., 2013, ES&T). Although, one limitation of the RPLC/DAD method is that we might be biased to certain molecular weights of BrC components. Prof. Cora Young's papers showed (especially Di Lorenzo et al., 2016, GRL) that SEC-UV is very good at resolving large molecular weight (MW) species, especially greater than 500 Da. Thus, we are biased to smaller MW species due to the use of RPLC. However, we can measure freshly-generated BrC components in the lower MW range and likely are missing the detection of larger species (especially > 1000 Da) either since they don't ionize or possibly were retained permanently by the PRLC column. With that said, we can still explore relative changes between fuel types and conditions with the compounds we report.

Reviewer Comment

In the non-targeted analysis, the use of retention time is not clear to me. Is it used to help propose a chemical formula for a given ion peak? Or page 7 it says similar m/z with difference were combined.

Authors response

The purpose of the non-targeted analysis is to efficiently reveal the differences between two spectra (e.g., "fresh" vs. "aged"). The BBOA constituents, as the detected/resolved ions shown in the SI section, were then carefully examined in the MassHunter with their exact m/z values, retention times (RTs), and peak areas. When examined by MassHunter, some chromatographic peaks had similar m/z values (usually within ±0.001 Da), resulting in the exact same molecular ion compositions. This indicated that these chromatographic peaks were likely isomers of each other, and thus, their peak areas were summed together in order to see how this molecular ion composition varied as a function of BB aerosol generation conditions. These data are recorded in the six tables of the SI (spreadsheet) Section. The chemical formulas were suggested based on the exact masses measured by the ESI-HR-QTOFMS. RTs reported in these tables from the RPLC separations provide information on hydrophobicity, where the later eluting components are more methanol soluble than water soluble. As noted earlier for the gradient elution method, components eluting in the first 2 minutes of the RPLC run are mostly water soluble since the mobile phase is solely composed of the aqueous eluent.

Changes made in the manuscript

To clarify the statement on page 7 the following will be added:

"When examined by MassHunter, the chromatographic peaks with similar *m/z* values (usually within ±0.001 Da) were found to have the same molecular formulas. This indicated that these chromatographic peaks were likely isomers of each other."

Reviewer Comment

Also, were any standard run to determine the expected retention time?

Authors response

*As described in Section 2.4, seven external (2-nitrophenol, 4-nitro-1-naphthol, 4-methyl-5-nitrocatechol, vanillin, vanillic acid, coniferaldehyde, and benzoic acid) commercially-available authentic standards were prepared for 6-point calibration curves from 0.004 –10 μg mL^{-1}, in order to obtain their retention times, as well and response factors and potential MS/MS fragments if needed. While this statement was in the context of previous studies, these standard were also run during these experiments. In addition, commercially-available authentic samples of 4-nitro-*o*-cresol and sinapinic acid were also run as external standards.*

The suggested names were listed in the six tables in SI (spreadsheet) are examples corresponding to the previously identified BBOA molecular formulas in the literature. For example, two isomers of m/z 161.0244 corresponding to $C_9H_6O_3$ (RT=8.32, 8.45) were suggested to be umbelliferone (Fleming et al. 2020) or hydroxycoumarin (Budisulistiorini et al. 2017). For compounds that were identified based on their high-resolution m/z *and retention time, these assignments have been denoted in the tables with a dagger* (†) *and their corresponding retention times in SI have been bolded. Descriptive text pertaining to this has been added to the table captions.*

Reviewer Comment

Or is a standard C18 elution program being used and a database of retention times being referenced?

Authors response
A standard elution program was used, as described in Section 2.3, but a database of retention times was not used. Retention times were used to determine the number of isomers present, but were not used explicitly for structural identification. Accurate mass analysis, previous observations in the literature, and lignin structural motifs were used to make suggested identifications shown in SI Tables. (spread sheet)

No database of retention times is being referenced here; however, compounds can be unequivocally identified to one of our 9 external standards.

Reviewer Comment
The UV/vis absorption spectra in Fig 5. These very flat featureless spectra do not make sense or provide any information. Even black carbon does not have such a flat wavelength spectrum. It seems that the UV/Vis absorption spectrum is averaged over the entire chromatogram. Why? This is throwing away valuable information, and likely explains why the spectra in Fig. 5 are so featureless. If you examine the absorption spectra for specific chromatographic peaks you can then relate the light absorption properties and potential chromophores to the ions observed at that same retention time. This provides molecular-level understanding of the specific compounds that are light absorbing, their sources, and their alteration by aging.

Authors response
UV/Vis absorption spectrum was averaged over the entire chromatogram, as described in Section 2.6.

The reviewer brings up a very good point. Considering this, a discussion of this has been added in the form of Section 3.4, the conclusion, and SI, as stated below. This includes figures such as Figure 6, where we demonstrate that we can chromatographically resolve some individual BrC components in the RPLC/DAD.

Changes to the Text

The following has been added following Section 3.3:

3.4 Chromatographic analysis of potential chromophores in the visible

In addition to examining the integrated spectrum, we can also focus on potential chromophores that absorb in the 500 – 570 nm region of the spectrum. Considering that flaming-dominated combustion shows little in the way of absorbing species and the abundance of these species decreases upon aging, only fresh emissions from combustion at 500 °C will be examined. Figure 6 shows the extracted wavelength chromatogram for the 500 – 510 nm region, where absorption would be most intense over this range, for Eucalyptus and Acacia combusted at 500 °C. This chromatogram has been background subtracted by the filter blank and, given that the amount of aerosol deposited on these filters was not measured, no scaling was applied.

Remarkably, only a few peaks dominate the chromatogram, though there are likely several low abundance and indistinct peaks 11 – 13 minutes. The UV/visible absorption spectra for each designated peak in Figure 6 are given in Figure S4. As can be seen in Figure 6, several of these species have similar retention times. A comparison was made between these peaks, with respect to elution time. Peak A and H, despite coming from different fuels, show similar retention times and UV spectra, as can be seen in Figure S5. The same can be said for peaks B, C, I, and J, which have well separated peaks at ~340 and ~485 nm with a gradual decrease to 600 nm. Peaks D, E, and K also have the same general appearance, and may be related to B, C, I and J, but are somewhat broader and peak at slightly shorter wavelengths (332 and ~480 nm).

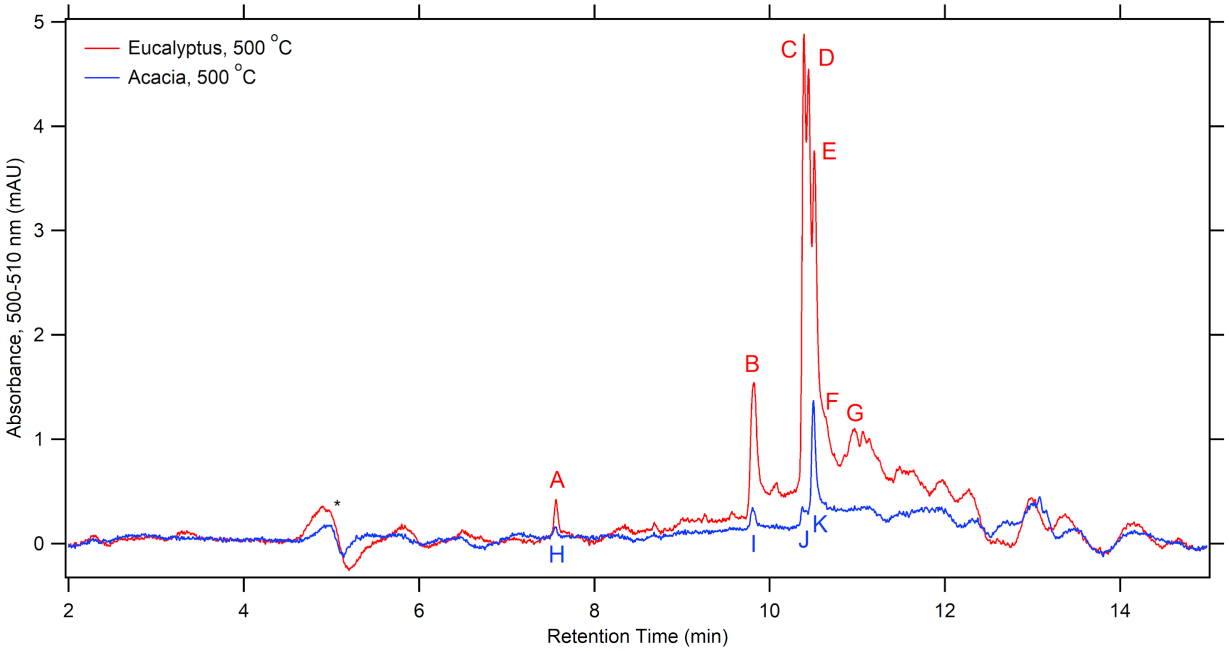

Figure 6. The extracted wavelength chromatogram for the 500 – 510 nm region for each fuel freshly combusted at 500 °C. The peak with the asterisk is an artifact from background subtraction.

To determine which species produced the absorption features shown in Figure 6, mass spectra at the absorption maxima were examined and assessed based on the peak height in the mass spectra, how well the retention times of extracted ion chromatograms matched the extracted visible wavelength chromatogram, and if a compound can be reasonably thought to absorb in the 500-510 nm region. Assignments using this method are tenuous, given that species detected by the DAD may not be seen by negative-mode ESI-MS. Additionally, many of the species described below have additional peaks outside those described, suggesting that not all isomers corresponding to a given formula absorb in this region. The extracted ion and visible chromatograms (shown in Figure 6) are in Figure S6a for Eucalyptus. Peak A is either $C_9H_{10}O_3$ (*m/z* 165.0559), tentatively assigned earlier, and/or $C_9H_{12}O_4$ (*m/z* 183.0658), which could be an isomer of trimethoxyphenol or dimethoxy methyl catechol. Several isomers of $C_9H_{10}O_3$ are known to only absorb below 240 nm, though veratraldehyde and caffeyl alcohol UV/visible spectra have not been measured, nor has trimethoxyphenol or dimethoxy methyl catechol for $C_9H_{12}O_4$. A $C_9H_{10}O_3$ isomer may also contribute to peak B and, while $C_8H_{10}O_2$ (*m/z* 137.0612) is more abundant at peak B and previously identified as several isomers in this work, none would absorb in this region. Likewise, $C_{10}H_{10}O_2$

(*m/z* 161.0604) elutes with peak B, which may be methoxycinnamaldehyde, methylcinnamic acid, or methylhydrocoumarin. While the spectra of those compounds have not been previously measured, it is unlikely that they would absorb in this region either. One compound that could weakly absorb in the visible and elutes at peak B is hydroxycoumarin ($C_9H_6O_3$, *m/z* 161.0244). One such compound, umbelliferone, absorbs to ~420 nm (Abu-Eittah and El-Tawil, 1985), though several isomers are present which may have somewhat different spectra.

Several species show peaks in the mass chromatogram that correspond to peaks B-F, including $C_{10}H_8O_3$ (*m/z* 175.0405), $C_{11}H_8O_3$ (*m/z* 187.0401), and $C_{11}H_{10}O_3$ (*m/z* 189.0565). The species corresponding to $C_{10}H_8O_3$ could be methoxycoumarin or methylhydroxycoumarin, though these species mainly absorb below ~450 nm (Abu-Eittah and El-Tawil, 1985) and may only absorb very weakly above 500 nm if at all. Naphthalenetriol is a much more likely candidate for $C_{10}H_8O_3$, given its extended and functionalized aromatic system, though a spectrum for any of its isomers has not been measured. The less functionalized 1,4-naphthalenediol absorbs to ~680 nm (Linstrom and Mallard, 2020). The structures attributable to $C_{11}H_8O_3$ could be hydroxynaphthoic acid, acetylcoumarin, or methylcoumarinaldehyde, but none of these compounds absorb above 410 nm (Donovalová et al., 2012). Still, several of these compounds are yellow solids in their pure forms according to their SDS sheets, suggesting they have some interaction with visible light. Similarly, an indistinct number of peaks associated with $C_{11}H_{10}O_3$ are found within these retention times, which may be isomers of methylmethoxycoumarin or dimethylhydroxycoumarin; none of which have previously measured spectra. Peaks in the vicinity of peaks F and G correspond to $C_{12}H_{10}O_3$ (*m/z* 201.0554) methoxynaphthoic acid or methoxyhydroxynaphthaldehyde. No UV/visible spectra are available for these compound and, while some spectra are available for related compounds such as 1- and 2-naphthoic acid (Linstrom and Mallard, 2020), these spectra seem truncated at ~350 nm. More telling is the SDS descriptions for these substituted naphthaldehydes and naphthoic acids, which are light yellow, yellow, and light brown. This suggest that their absorption extends into the visible and possibly into the 500 nm region.

One set of isomers in the vicinity of peaks C through F correspond to the formula of $C_{11}H_6O_3$ (*m/z* 185.0256). Given the high degree of unsaturation (DBE = 9), these can only be furanocoumarins, which have a fused furan and benzene ring. Two common isomers of these species are psoralen and angelicin. While these species do not absorb in this region of this visible, they are strong absorbers below 370 nm (Rutan et al., 2018) and have not been previously identified as BrC species in BB aerosol. The peaks for nitroguaiacol, discussed earlier in this work, do not align well with peaks in Figure 6.

Fresh Acacia combusted at 500 °C underwent a similar analysis, as shown in Figure S6b. All the previously mentioned extracted ion chromatograms appear very similar for Acacia, with the main difference being that the ion abundance for Acacia was smaller by a factor or 2-4. Most ions had similar temporal profiles as Eucalyptus except for $C_{11}H_{10}O_3$ (*m/z* 189.0565), which only matched peak K and onwards. Given this, it is very likely that peaks with similar DAD retention times are produced by the same species, and peak A corresponds with peak H, B with I, C with J, and E with K.

The following has been added to the Conclusion section:

"An attempt was also made to identify which species produce absorption at wavelengths longer than 500 nm. An extracted wavelength chromatogram from 500 – 510 nm shows only a few peaks dominate the absorption from fresh emissions of combustion at 500 °C. Both Acacia and Eucalyptus have common absorbing species, as shown by peaks with common retention times, similar UV/Visible spectra, and extracted ion chromatograms. By comparing the retention times of extracted ion and wavelength chromatograms, several species were tentatively suggested for contributing to absorption in this wavelength range. This includes functionalized courmarin species (hydroxy-, methoxy- methylhydroxy-, methylmethoxy-, etc.), naphthalenetriol, and methoxyhydroxynaphthaldehyde or methoxynaphthoic acid. UV spectra available from the literature for several of these species and/or related compounds seem truncated and are very likely to extend into this visible region of the spectrum, which highlights the need for broadband UV/Visible spectral measurements of these compounds. While not important for absorption in this visible region, a novel set of compounds were found that could be strong BrC species – furanocoumarins."

The following Figures have been added to the Supplemental Information:

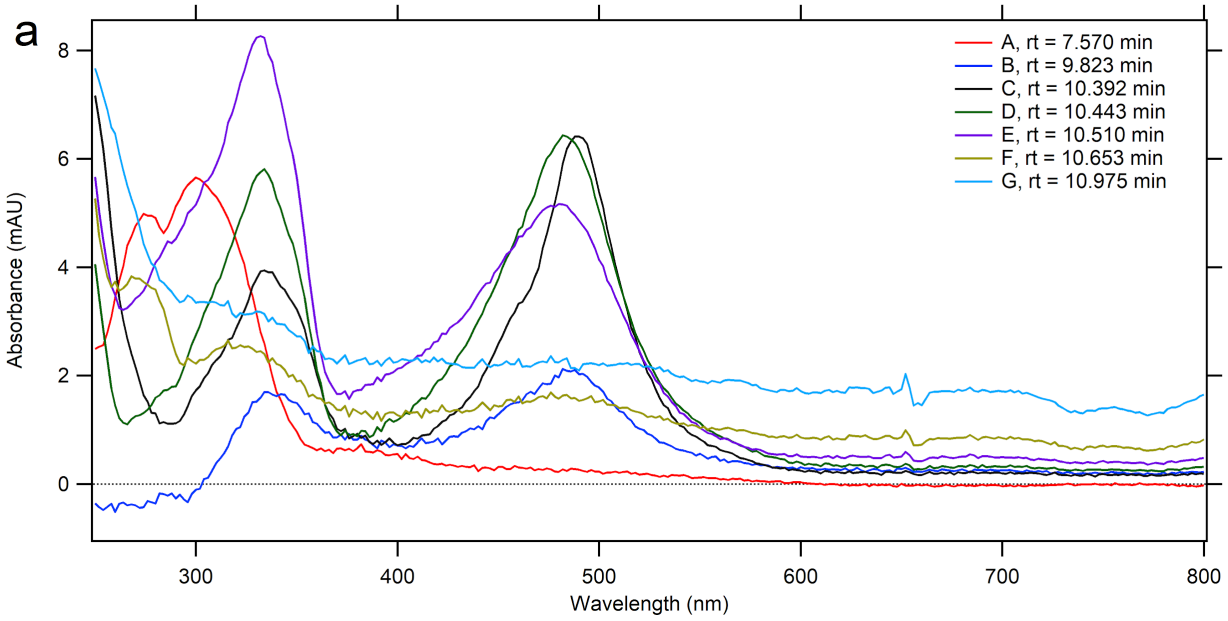

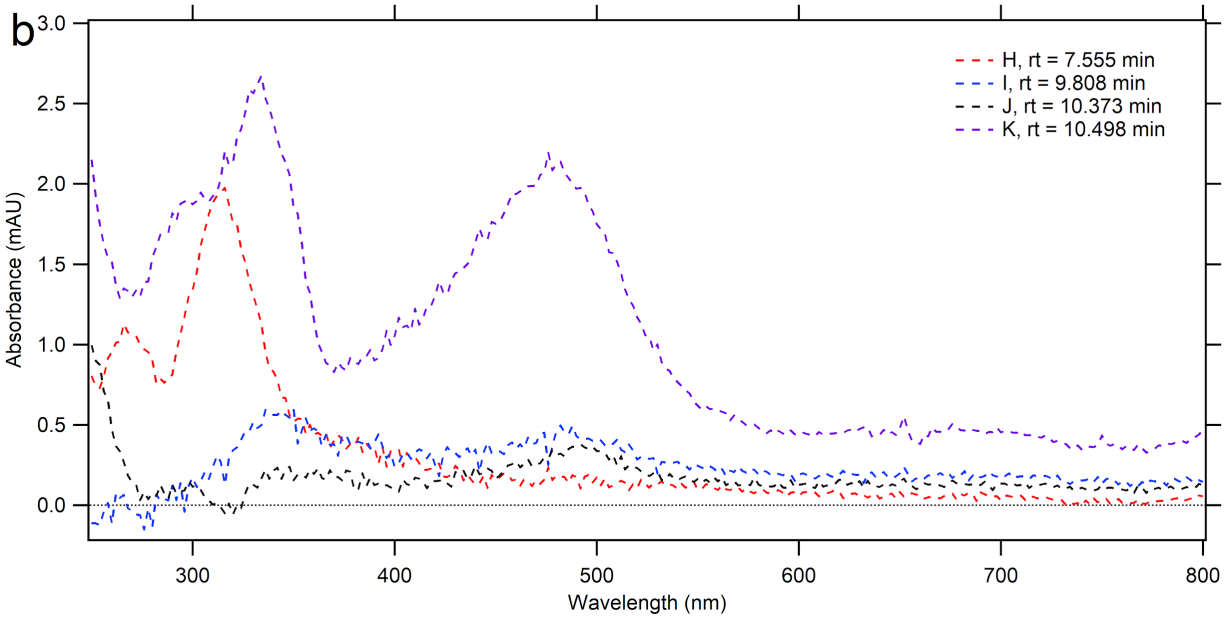

Figure S4. The UV/Visible absorption spectra corresponding to peaks in Figure 6, with those associated with Eucalyptus plotted with solid lines and those associated with Acacia with dashed lines. Peaks were background subtracted against nearby "off-peak" retention times; specifically, 7.62 min for peak A, 9.717 min for peak B, 10.312 min for peaks C-G, 7.483 min for peak H, 9.726 min for peak I, and 10.323 min for peaks J and K. As can be seen in Figure 6, a nearby retention time free of absorbers in the 500-510 region was not always readily available, so caution should be used when utilizing these spectra.

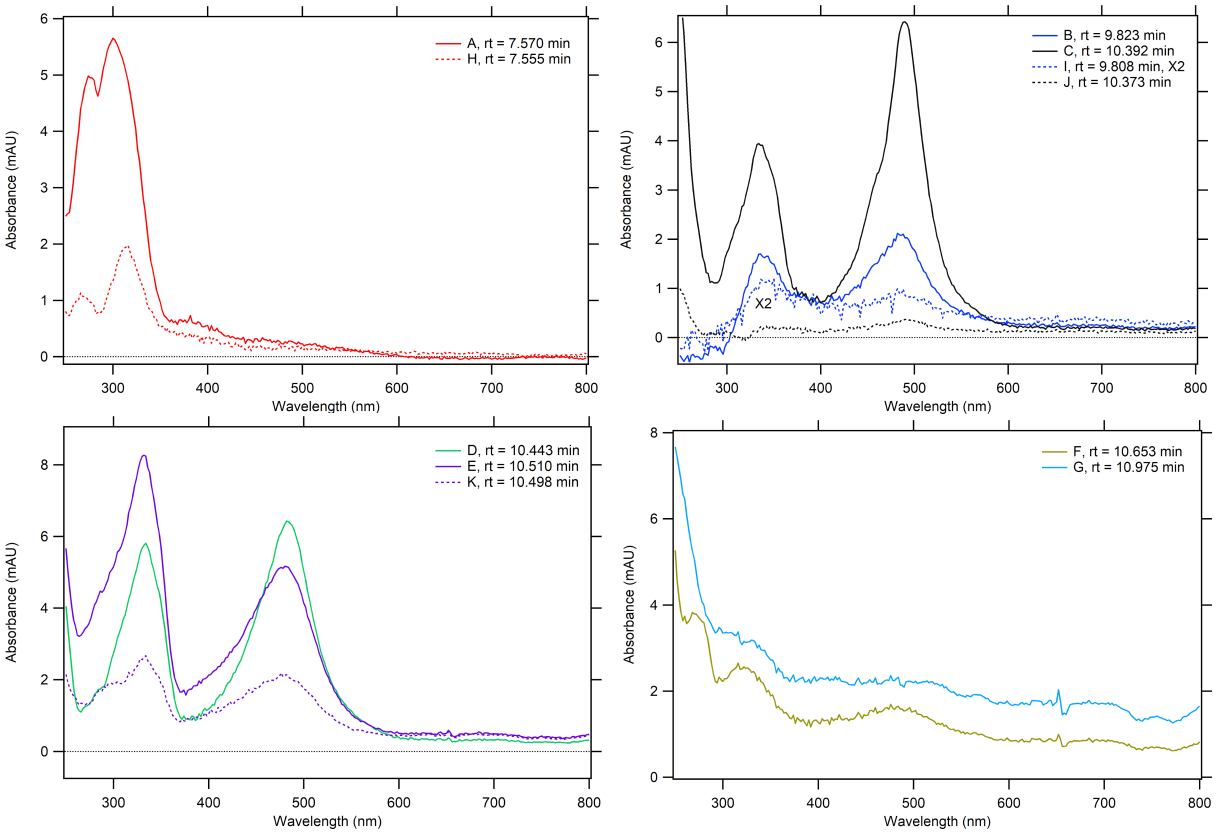

Figure S5. Similar to Figure S4, only with a pairwise comparison of species with similar retention times between the Acacia and Eucalyptus sample when combusted at 500 °C.

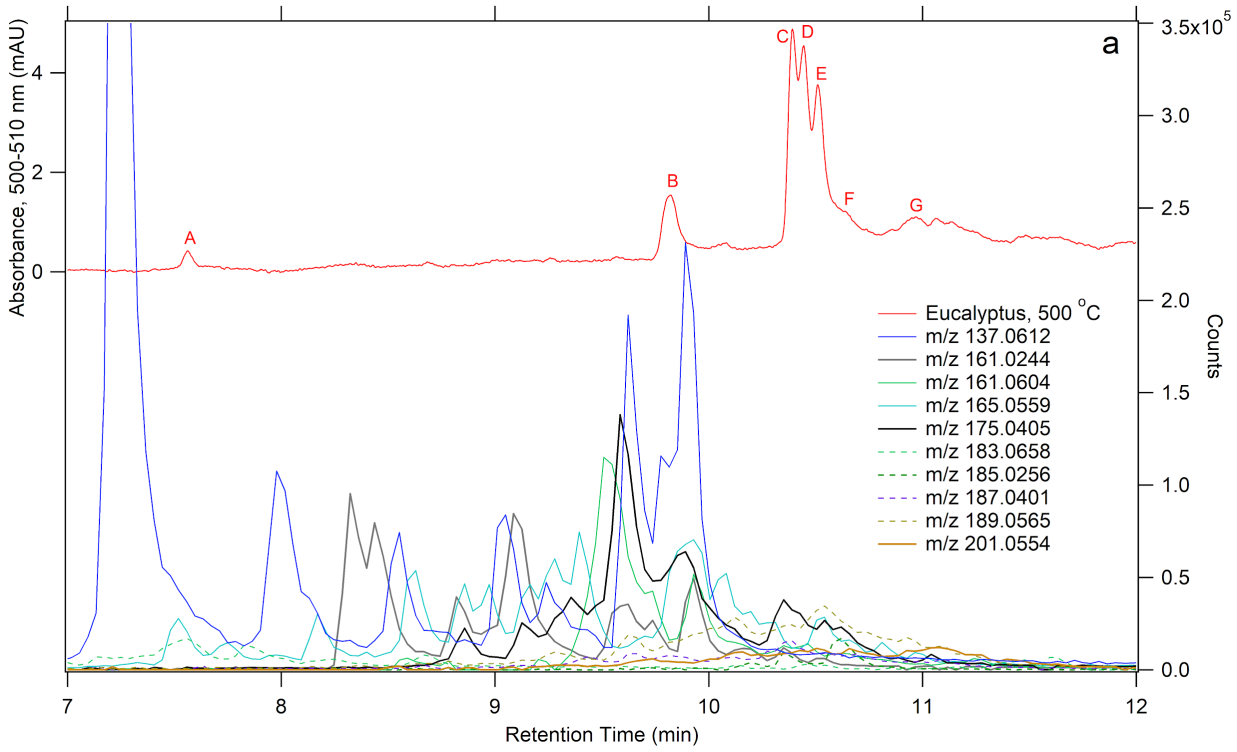

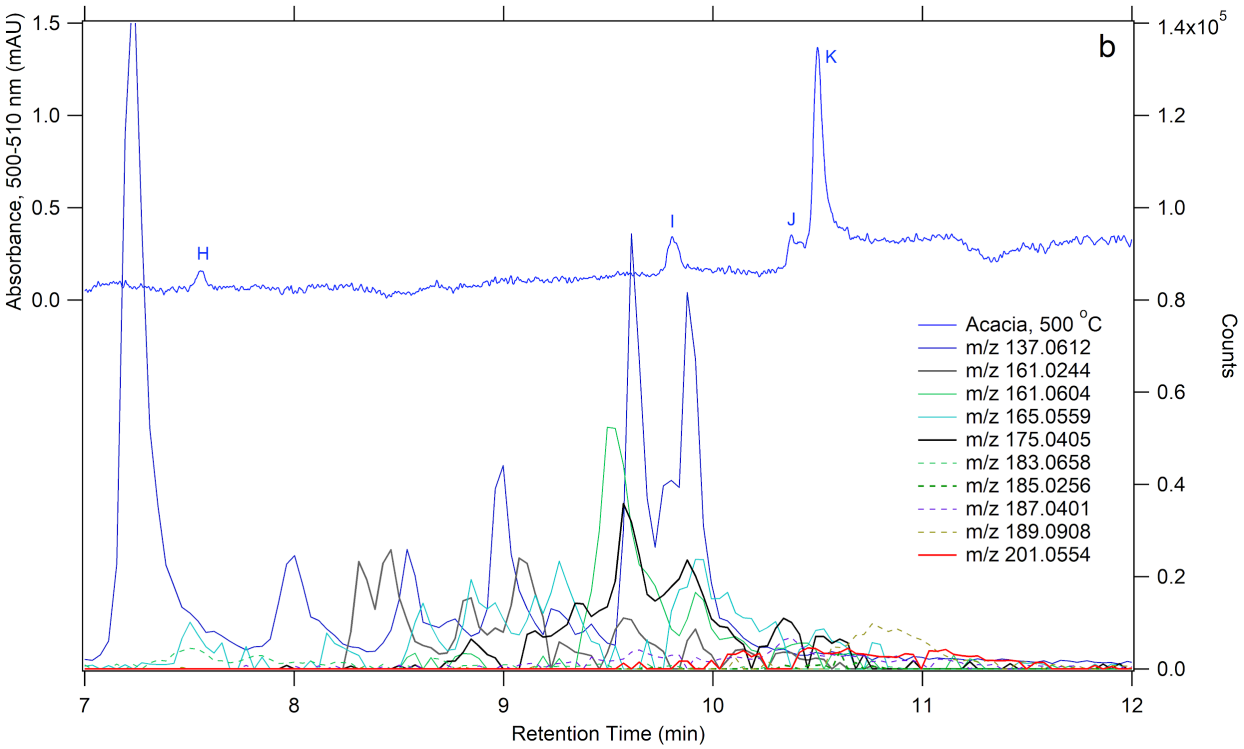

Figure S6. Extracted ion chromatograms for (a) Eucalyptus and (b) Acacia, which have chromatographic features matching the UV/Visible chromatogram for 500-510 nm. Ion chromatograms in bold are likely strong absorbers according to our analysis.

Reviewer Comment

Throughout the paper brown carbon (BrC) is discussed as though it is a distinct component, but it is just the organic carbon that has a significant molar absorptivity or real refractive index in the UV/vis wavelengths of interest. There is plenty of evidence from prior studies that BrC cannot be separated or easily distinguished from the rest of the organic aerosol. It really exists as a spectrum. See for example Rawad Saleh's work on this topic.

Authors response

Several studies have shown that BrC cannot be separated or easily distinguished from the rest of the organic aerosol. The optical properties of primary and secondary BrC span a wide range of values, inherent to broad variability in its chemical composition, mixing states of individual particles and their dynamic transformations resulting from atmospheric aging. Therefore, unraveling the relationship between the light-absorbing properties of BrC and its composition requires the use of a variety of complementary analytical techniques to determine both bulk and molecular-specific BrC properties [1-6]. But for biomass burning emissions, for lower MCE (< 0.9), the fraction of BC is very low (below 10% or so), whereas for higher MCE (>0.98), the fraction of BC is significantly higher. So, we still think we can say that less BC is produced during smoldering combustion, whereas more BC is produced during flaming combustion as in previous studies [7-11]. Indeed, Saleh classified BrC into four optical regions as a continuum associated with a continuum of physicochemical properties, including molecular sizes, volatility, and

*solubility [12, 13]. We will state these facts and the current understanding to indicate the very narrow definition of the use of the word BrC used in this paper. The language used in this work about BrC was mainly to contrast it with BC, which is decidedly a different component of aerosol, even if inextricably mixed in BBA. However, we disagree with the reviewer's statement "*There is plenty of evidence from prior studies that BrC cannot be separated or easily distinguished from the rest of the organic aerosol" *as our analysis shown in Figure 6 above we can resolve constituents that are BrC.*

Changes Made in the Manuscript

The following is added

"Several recent studies have shown that BrC cannot be separated or easily distinguished from the rest of the organic aerosol (Saleh, 2020). BrC is classified into four optical regions as a continuum associated with a continuum of physicochemical properties, including molecular sizes, volatility, and solubility(Saleh et al., 2018;Saleh, 2020) . The language used in this work for BrC was mainly to contrast it with BC, based on the combustion temperature, which is decidedly a different component of aerosol, even if inextricably mixed in BBA."

1. Bluvshtein, N.; Lin, P.; Flores, J. M.; Segev, L.; Mazar, Y.; Tas, E.; Snider, G.; Weagle, C.; Brown, S. S.; Laskin, A.; Rudich, Y., Broadband optical properties of biomass-burning aerosol and identification of brown carbon chromophores. Journal of Geophysical Research-Atmospheres 2017, 122 (10), 5441-5456.
2. Flores, J. M.; Washenfelder, R. A.; Adler, G.; Lee, H. J.; Segev, L.; Laskin, J.; Laskin, A.; Nizkorodov, S. A.; Brown, S. S.; Rudich, Y Complex refractive indices in the near-ultraviolet spectral region of biogenic secondary organic aerosol aged with ammonia. Physical Chemistry Chemical Physics 2014, 16 (22), 10629-10642.
3. Brown, S. S.; George, C.; Laskin, A.; Rudich, Y., Formation of Secondary Brown Carbon in Biomass Burning Aerosol Proxies through NO3 Radical Reactions. Environmental Science & Technology 2020, 54 (3), 1395-1405.
4. Li, C. L.; He, Q. F.; Schade, J.; Passig, J.; Zimmermann, R.; Meidan, D.; Laskin, A.; Rudich, Y., Dynamic changes in optical and chemical properties of tar ball aerosols by atmospheric photochemical aging. Atmospheric Chemistry and Physics 2019, 19 (1), 139-163.
5. Lin, P.; Bluvshtein, N.; Rudich, Y.; Nizkorodov, S. A.; Laskin, J.; Laskin, A., Molecular Chemistry of Atmospheric Brown Carbon Inferred from a Nationwide Biomass Burning Event. Environmental Science & Technology 2017, 51 (20), 11561-11570.
6. Xu, J. Z.; Hettiyadura, A. P. S.; Liu, Y. M.; Zhang, X. H.; Kang, S. C.; Laskin, A., Regional Differences of Chemical Composition and Optical Properties of Aerosols in the Tibetan Plateau. Journal of Geophysical Research-Atmospheres 2020, 125 (1).
7. Lewis, K., Arnott, W. P., Moosmüller, H., and Wold, C. E.: Strong spectral variation of biomass smoke light absorption and single scattering albedo observed with a novel dual-wavelength photoacoustic instrument, Journal of Geophysical Research: Atmospheres, 113, 10.1029/2007jd009699, 2008.
8. Liu, S., Aiken, A. C., Arata, C., Dubey, M. K., Stockwell, C. E., Yokelson, R. J., Stone, E. A., Jayarathne, T., Robinson, A. L., DeMott, P. J., and Kreidenweis, S. M.: Aerosol single

scattering albedo dependence on biomass combustion efficiency: Laboratory and field studies, Geophysical Research Letters, 41, 742-748, 10.1002/2013GL058392, 2014.
9. McMeeking, G. R., Fortner, E., Onasch, T. B., Taylor, J. W., Flynn, M., Coe, H., and Kreidenweis, S. M.: Impacts of nonrefractory material on light absorption by aerosols emitted from biomass burning, Journal of Geophysical Research: Atmospheres, 119, 12,272-212,286, 10.1002/2014jd021750, 2014.
10. Pokhrel, R. P., Wagner, N. L., Langridge, J. M., Lack, D. A., Jayarathne, T., Stone, E. A., Stockwell, C. E., Yokelson, R. J., and Murphy, S. M.: Parameterization of single-scattering albedo (SSA) and absorption Ångström exponent (AAE) with EC / OC for aerosol emissions from biomass burning, Atmos. Chem. Phys., 16, 9549-9561, 10.5194/acp-16-9549-2016, 2016.
11. Stockwell, C. E., Christian, T. J., Goetz, J. D., Jayarathne, T., Bhave, P. V., Praveen, P. S., Adhikari, S., Maharjan, R., DeCarlo, P. F., Stone, E. A., Saikawa, E., Blake, D. R., Simpson, I. J., Yokelson, R. J., and Panday, A. K.: Nepal Ambient Monitoring and Source Testing Experiment (NAMaSTE): emissions of trace gases and light-absorbing carbon from wood and dung cooking fires, garbage and crop residue burning, brick kilns, and other sources, Atmos. Chem. Phys., 16, 11043-11081, 10.5194/acp-16-11043-2016, 2016.
12. Saleh, R., From Measurements to Models: Toward Accurate Representation of Brown Carbon in Climate Calculations. Current Pollution Reports 2020, doi: 10.1007/s40726-020-00139-3.
13. Rawad Saleh, Zezhen Cheng, and Khairallah Atwi:The Brown−Black Continuum of Light-Absorbing Combustion Aerosols,: Environ. Sci. Technol. Lett. 2018, 5, 508−513

Reviewer Comment

The role of catechol is mentioned and there has been much recent work on the role of nitration of catechol as well as other aqueous chemistry in producing BrC. This needs to be discussed and in order to do so a solid understanding of the NOx/NOy chemistry in the fresh and aged BBA must be determined and presented. Biomass burning typically emits substantial NOx, and NOy such as HONO.

Authors response

The focus of this work has been on determining which species are most affected by aging and how the changes in molecular constituents alter the optical properties of aerosol. Given the complexity of the system, we have addressed the mechanistic aspects of production and removal in only a limited sense. However, given the abundance of catechol and how significantly it changes upon aging, we agree with the reviewer that a more in-depth discussion of this and related compounds is warranted.

Changes to Manuscript

The following has been added to the end of Section 3.2:

"Given that one isomer of dihydroxybenzene undergoes the greatest change upon aging, it is worth examining potential chemical transformations further. While resorcinol is a potential identity, catechol has gained significant attention due to its involvement as a precursor to a strong chromatophore. Catechol can react in the atmosphere to form 4-nitrocatechol ($C_6H_5NO_4$) through photochemical and dark processes in the gas and aqueous phase through a number of mechanisms (Finewax et al., 2018; Kroflič et al., 2018; Vidovic et al., 2018; Wang et al., 2019). Given the

dryness of our chamber and the presence of UV irradiation, this mechanism would proceed through hydrogen abstraction from the hydroxyl by OH to produce a *β*-hydroxyphenoxy/*o*-semiquinone radical, followed by radical-radical combination with NO_2 (Finewax et al., 2018). Both fresh and aged spectra for 500 °C combustion were examined for nitrocatechol ($(M-H)^-$ at *m/z* 154.0140), and it was found at a rt of 8.39-8.55 min in both fresh and aged Acacia and Eucalyptus. There was a greater abundance in the aged samples, despite the mass loading on the filter being lower, suggesting a small amount from primary emission, but mainly a product of secondary formation for both fuels.

Smoldering-dominated burns were also examined for other nitroaromatic species. Methyl nitrocatechol, which has been identified as a tracer for BB SOA (Iinuma et al., 2010), and nitroguaiacol both have the formula of $C_7H_7NO_4$ and would have an $(M-H)^-$ peak at *m/z* 168.0297. Fresh Eucalyptus had two peaks at retention times of 7.71 and 9.31 min, while Acacia only had a single peak at 9.30 min. Using the exact mass and the rt, this peak at 9.30 min has been identified as 4-methyl-5-nitrocatechol, so the 7.71 min peak must be another isomer produced in fresh combustion. Since this compound must be more polar to elute earlier, it may be the 4-, 5-, or 6-isomer of nitroguaiacol (Bluvshtein et al., 2017; Kitanovski et al., 2012a). Upon aging, both fuels had two peaks with smaller absolute abundances at 9.5-9.6 and 10.0 min. The 9.5-9.6 min peak is likely a slightly shifted 4-methyl-5-nitrocatechol, suggesting both a primary and secondary source of the compound. Based on previous observations of BB aerosol, the 10.0 min peak is either 3-methyl-6-nitrocatechol, 3-methyl-5-nitrocatechol, or 4-nitroguaiacol, whose sensitivity can be altered for it to elute either before or after 4-methyl-5-nitrocatechol (Bluvshtein et al., 2017;Kitanovski et al., 2012a). Nitrophenol ($C_6H_5NO_3$, $(M-H)^-$ at *m/z* 138.0191) and nitrocresol ($C_7H_7NO_3$, $(M-H)^-$ at *m/z* 152.0348) are secondary products of phenol and cresol, respectively. Neither was observed for fresh Eucalyptus and Acacia. There are at least two forms of methyl nitrophenol in aged Acacia (rt of 10.15 and 10.46 min) and only one (rt 10.47 min) in aged Eucalyptus. Several isomers have been observed in BB aerosol in previous studies, including 3-methyl-4-, 2-methyl-4-, and 2-methyl-6-nitrophenol (Bluvshtein et al., 2017; Kitanovski et al., 2012a). The peak with a rt of ~10.46 was likely a slightly shifted 4-nitro-*o*--cresol, which was a standard compound run during the analysis of fresh BB aerosol and had a rt of 10.30 min. One nitrophenol peak at 9.37 min was observed in aged Acacia, while aged Eucalyptus did not exhibit any nitrophenol. This had a different rt than the 2-nitrophenol standard, which had a rt of 10.05 min, suggesting it was some other isomer. Nitronaphthol ($C_{10}H_7NO_3$, $(M-H)^-$ at *m/z* 188.0348) was not observed in any spectra."

The following has been added to the conclusion section:
"The removal of dihydroxybenzene was investigated by examining spectra for a known reaction product, dihydroxynitrobenzene (e.g. nitrocatechol). Results for both fuels suggest a small amount was produced by primary emissions, but it was mainly a product of secondary formation… Focusing on nitroaromatic species, one isomer of nitrophenol was produced during the aging of Acacia combusted at 500 °C, while none was produced for Eucalyptus. Despite being thought of as a tracer for BB SOA (Iinuma et al., 2010), there is evidence for both primary emission and secondary production of 4-methyl-5-nitrocatechol."

Reviewer Comment
There are several inappropriate and unsupported statements made regarding particle morphology and its role in the light absorption properties. For example, on page 2 "BrC aerosols are spherical

in morphology", and on line 513: "Such an increase in SSA resulting from morphology changes is implausible". Aging can drive the condensation of secondary components that change morphology (how well coated the BC is, for example) that can absolutely alter SSA.

Authors response

Below are TEM images of particles produced from Eucalyptus for 500 °C and at 800 °C. combustion. They appear spherical, or nearly so, as at 500 °C (image B) as opposed to the images at 800 °C (image A)

Image A

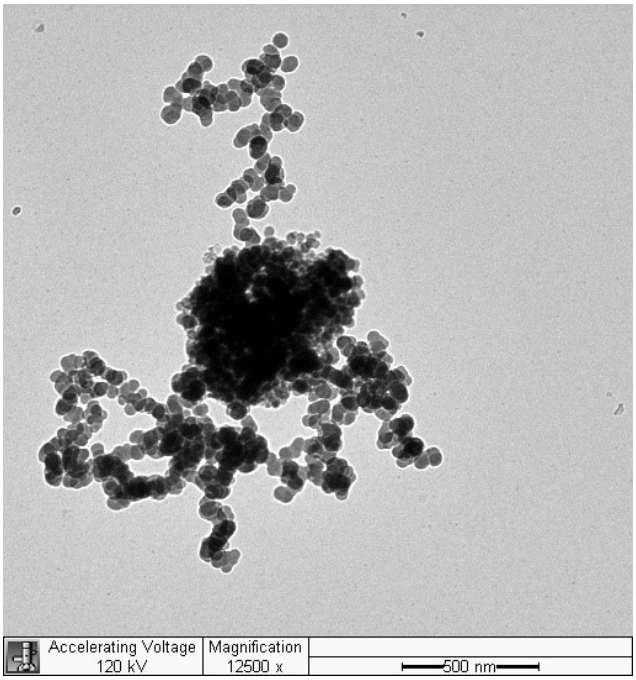

Image B

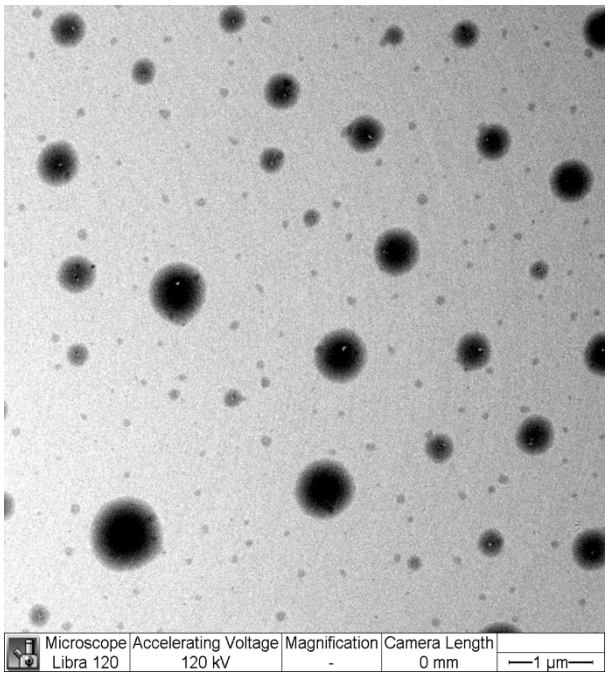

The authors agree that condensation can drive morphology changes, as has been demonstrated in numerous studies. Unlike previous work, however, the size-resolved measurements in this work mean that it is smaller particles that must gain secondary components. We make the "implausible" statement because it is very unlikely that only morphology changes can produce SSA changes of 0.3.

Changes to Manuscript

Line 515 now states that "Such an increase in SSA resulting from morphology changes alone seems implausible…"

Reviewer Comment

More details on the type of TEM grid and how the sample was collected on it are required. Is it coated with formvar or similar, or a bare metal grid?

Authors response

The authors apologize, as it seems another digit was put into the part number. This has been corrected and detail added.

Changes to Manuscript
The text now reads "BB aerosols were collected onto 47-mm Teflon filters (Tisch Environmental, SF18040) for chemical analysis and tunneling electron microscope (TEM) grids (Ted Pella, 01844, carbon film on 400 mesh copper) for image analysis."

Reviewer Comment
Flaming-phase combustion also increases the mass fraction of inorganic components present, and nitrogen oxides and chloride can play a role in BrC chemistry (line 331). Were the inorganic components measured and quantified?

Authors response
No.

Reviewer Comment
Line 573: What mass fraction of eucalyptol would have to be present to explain the observations? Is this reasonable?

Authors response
The reason the authors hypothesize its presence is that it can make up a large, if not the majority, of distillation products. While we understand the importance of the reviewer's request and the refractive index has been measured near this region (Monerie, et al. 1985), there are several reasons we are hesitant to make this assessment. First, it was not directly measured, so its presence is conjectural. Secondly, while we have done Mie and RDG calculations in the past, we are not currently set up to do core-shell calculations, which would be needed to properly address this comment. In short, the authors are not comfortable making such an assessment based on its conjectured presence. In order to bolster the statement in the paper, the text will be accentuated.

Changes to Manuscript
The following has been added to line 359, where eucalyptol is first mentioned:
"When extracting essential oil from Eucalyptus leaves by water-steam distillation, an oil yield of 0.3 – 2.0% (dry wt.) was produced of which 7 – 75% was eucalyptol, depending on the species (Masamba et al., 2001; Subramanian et al., 2012)."

References

Abu-Eittah, R. H. and B. A. H. El-Tawil (1985). "The electronic absorption spectra of some coumarins. A molecular orbital treatment." Canadian Journal of Chemistry 63(6): 1173-1179.

Anjum, N., et al. (2015). "Impact of drying methods on content and quality of essential oil from leaves of Artemisia nilagirica (clarke) pamp." World J. Pharm. Pharm. Sci. 4(9): 1259-1271.

Bluvshtein, N.; Lin, P.; Flores, J. M.; Segev, L.; Mazar, Y.; Tas, E.; Snider, G.; Weagle, C.; Brown, S. S.; Laskin, A.; Rudich, Y., Broadband optical properties of biomass-burning aerosol and identification of brown carbon chromophores. Journal of Geophysical Research-Atmospheres 2017, 122 (10), 5441-5456.

Bordin, F., et al. (1991). "Angelicins, angular analogs of psoralens: Chemistry, photochemical, photobiological and phototherapeutic properties." Pharmacology & Therapeutics 52(3): 331-363.

Budisulistiorini, S. H.; Riva, M.; Williams, M.; Chen, J.; Itoh, M.; Surratt, J. D.; Kuwata, M. Light-Absorbing Brown Carbon Aerosol Constituents from Combustion of Indonesian Peat and Biomass. Environ. Sci. Technol. 2017, 51 (8), 4415–4423. https://doi.org/10.1021/acs.est.7b00397

Fleming, L. T.; Lin, P.; Roberts, J. M.; Selimovic, V.; Yokelson, R.; Laskin, J.; Laskin, A.; Nizkorodov, S. A. Molecular Composition and Photochemical Lifetimes of Brown Carbon Chromophores in Biomass Burning Organic Aerosol. Atmos. Chem. Phys. 2020, 20 (2), 1105–1129. https://doi.org/10.5194/acp-20-1105-2020.

Kitanovski, Z., et al. (2012). "Liquid chromatography tandem mass spectrometry method for characterization of monoaromatic nitro-compounds in atmospheric particulate matter." Journal of Chromatography A 1268: 35-43.

Lin, P.; Fleming, L. T.; Nizkorodov, S. A.; Laskin, J.; Laskin, A. Comprehensive Molecular Characterization of Atmospheric Brown Carbon by High Resolution Mass Spectrometry with Electrospray and Atmospheric Pressure Photoionization. Anal. Chem. 2018, 90 (21), 12493–12502. https://doi.org/10.1021/acs.analchem.8b02177.

Masamba, W. R. L., et al. (2001). "Composition and properties of essential oils from Eucalyptus camaldulensis and E. tereticornis." Malawi J. Sci. Technol. 6: 81-89.

Monerie, M., et al. (1985). "Refractive-index measurements of 1,8-cineole (eucalyptol) in the 0.6-1.7-μm range." Appl. Opt. 24(7): 990-993.

Subramanian, P. A., et al. (2012). "Yield, contents and chemical composition variations in the essential oils of different Eucalyptus globulus trees from Tigray, Northern Ethiopia." J. Pharm. Biomed. Sci.(17): 11.

Laboratory studies of fresh and aged biomass burning aerosol emitted from east African biomass fuels - PART 2 - Chemical properties and characterization

Damon M. Smith,[1,2,#] Tianqu Cui,[4,&] Marc N. Fiddler,[3] Rudra Pokhrel,[1] Jason D. Surratt,[4] Solomon Bililign[1*]

1. Department of Physics, North Carolina Agricultural and Technical State University, Greensboro, NC, 27411 USA,
2. Applied Sciences and Technology Program, North Carolina A&T State University, Greensboro, NC 27411, USA,
3. Department of Chemistry, North Carolina Agricultural and Technical State University, Greensboro, NC, 27411, USA
4. Department of Environmental Science and Engineering, Gillings School of Global Public Health, University of North Carolina, Chapel Hill, NC, 27599 USA

Current Address: Department of Chemistry and Physics, Western Carolina University, Cullowhee, NC 28723
& Current Address: Laboratory of Atmospheric Chemistry, Paul Scherrer Institute, Villigen 5232, Switzerland
* Correspondence: Bililign@ncat.edu; Tel.: (+13362852328);

Abstract: There are many fuels used for domestic purposes in east Africa, producing a significant atmospheric burden of the resulting aerosols, which includes biomass burning particles. However, the aerosol physicochemical properties are poorly understood. Here, combustion of Eucalyptus, Acacia, and Olive fuels were performed at 500 and 800 °C in a tube furnace, followed by immediate filter collection for fresh samples or introduction into a photochemical chamber to simulate atmospheric photochemical aging under the influence of anthropogenic emissions. The aerosol generated in the latter experiment was collected onto filters after 12 hours of photochemical aging. 500 and 800 °C were selected to simulate smoldering and flaming combustion, respectively, and to cover a range of combustion conditions. Methanol extracts from Teflon filters were analyzed by ultra-performance liquid chromatography interfaced to both a diode array detector and an electrospray ionization high-resolution quadrupole time-of-flight mass spectrometer (UPLC/DAD-ESI-HR-QTOFMS) to determine the light-absorption properties of biomass burning organic aerosol constituents chemically characterized at the molecular level. Few chemical or UV/Visible differences were apparent between samples for either fuel when combusted at 800 °C. Differences in single scattering albedo (SSA) between fresh samples at this temperature were attributed to compounds not captured in this analysis, with eucalyptol being one suspected missing component. For fresh combustion at 500 °C, many species were present, where lignin pyrolysis and distillation products are more prevalent in Eucalyptus, while pyrolysis products of cellulose and at least one nitroaromatic species were more prevalent in Acacia. SSA trends are consistent with this, particularly if the absorption of those chromophores extends to the 500 – 570 nm region. Upon aging, both show that resorcinol or catechol was removed to the highest degree, and both aerosol types were dominated by loss of pyrolysis and distillation products, though both differed in the specific compounds being consumed by the photochemical aging process.

Deleted: s

Deleted: and

Deleted: was

1 Introduction

This is the second part of a two-part laboratory measurement of optical and chemical properties of biomass burning (BB) aerosols emitted by east African fuels, focused on chemical properties. Biomass fuels were combusted at two different temperatures: Combustion at 500 °C corresponds to a smoldering-dominated fire, which leads to the formation of large quantities of molecular organic compounds and brown carbon (BrC) constituents in the resulting aerosol (Collier et al., 2016). These smoldering BB aerosols typically have modified combustion efficiency (MCE) values < 0.9. Combustion at 800 °C corresponds to a flaming-dominated fire that mainly forms black carbon (BC) aerosols (Reid et al., 2005), with MCE values > 0.9. Given the lack of MCE measurements in wildfires or in-cook stoves in east Africa, a range of combustion conditions were covered in this work. This also highlights the paucity of available measurements of combustion conditions in Africa and the need for such measurements, so that appropriate laboratory scale experiments can be performed.

A soot photometer aerosol mass spectrometer (SP-AMS) characterization of the chemical composition of BC-containing aerosol emitted by BB fuel sources was conducted during the Fire Lab at Missoula Experiments (FLAME) (McClure et al., 2019;May et al., 2014). The work focused on analyzing variations in the particle composition as a function of fuel and combustion conditions. Differences in the refractory black carbon (rBC) were observed with some fuel sources. Organic species were found to vary by orders of magnitude relative to rBC, depending on the fuel source. Chemical differences were also observed between the aged and fresh samples (Fortner et al., 2018).

A component of organic aerosol, BrC, has emerged as a significant type of BB aerosol. Also known as light-absorbing organic carbon, BrC in atmospheric particles has received much attention for its potential role in global radiative forcing (Qin et al., 2018). Primary organic aerosol (POA) contributes an estimated 10% of total solar absorption by BB aerosols, while aged OA contributes an estimated 30%, making secondary organic aerosol (SOA) production an important source of BrC (Kumar et al., 2018). As few as 20 −25 BrC chromophores are responsible for 40−50% of total UV absorbance in the 300 – 500 nm range (Laskin et al., 2018). While several field measurement campaigns have differentiated light absorption by BC and BrC, the chemical characteristics of BrC are not currently well understood (Qin et al., 2018).

BrC is often associated with emissions from incomplete combustion (Andreae and Gelencsér, 2006), but can also form via secondary reactions in the atmosphere (Laskin et al., 2015). Aerosol obtained from 500 °C burn classified as BrC aerosol are spherical in morphology as seen in the TEM images and are yellow-brown in color due to values of the imaginary portion of the refractive index (κ) that increase sharply toward shorter visible and ultraviolet wavelengths (Bond and Bergstrom, 2006). BrC is comprised of a wide range of poorly characterized compounds exhibiting highly variable light-absorption properties, with reported κ values spanning two orders of magnitude (Saleh et al., 2013;Chen and Bond, 2010;Kirchstetter et al., 2004;McMeeking et al., 2009). Its optical properties have been shown to change through atmospheric processing, such as oxidation, absorption of solar radiation leading to particle-phase reactions, and aqueous-phase processing within aerosol particles (Lambe et al., 2013;Lambe et al., 2011;Sareen et al., 2013;Lee et al., 2014;Zhao et al., 2015;Nguyen et al., 2012;Laskin et al., 2015).

Formatted: Superscript

Deleted: s

These factors make the chemical composition of BrC dependent on location and source of fuel (Laskin et al., 2015;Moise et al., 2015). Many BrC chromophores vary significantly among biomass species, although some, such as sinapaldehyde and coniferaldehye are common among certain types of biomass fuels, such as angiosperms and gymnosperms, respectively. Other chromophores depend on combustion conditions, such as vanillic acid, which has only been observed as a product of smoldering combustion, when the MCE is low (Fleming et al., 2019). Further, an effect known as photo-bleaching can occur, where POA chromophores can lose their absorptivity or be destroyed entirely when irradiated by UV light for several hours (Laskin et al., 2018). Since the light-absorption spectra of organic compounds is dependent on their molecular structure, identifying atmospheric chromophores making up BrC is essential for understanding the changes in aerosol optical properties (Moise et al., 2015;Kitanovski et al., 2012a;Mohr et al., 2013;Teich et al., 2017;Zhang et al., 2013). Several recent studies have shown that BrC cannot be separated or easily distinguished from the rest of the organic aerosol (Saleh, 2020). BrC is classified into four optical regions as a continuum associated with a continuum of physicochemical properties, including molecular sizes, volatility, and solubility(Saleh et al., 2018;Saleh, 2020) . The language used in this work for BrC was mainly to contrast it with BC, based on the combustion temperature, which is decidedly a different component of aerosol, even if inextricably mixed in BBA.

In the companion paper, Part I, we described the laboratory measurements of a fuel specific study of the optical properties of BB aerosol emitted by three different fuels sourced from east Africa (Smith et al., 2020). This study was conducted under different aging and combustion conditions using a tube furnace and indoor smog chamber. Optical properties were measured for BB aerosols produced under smoldering and flaming conditions for each fuel type. For each combustion condition, we reported the measured optical properties. These include scattering and extinction cross sections, single scattering albedo (SSA), absorption and extinction for fresh emissions, emissions aged in the dark and emissions photochemically aged in the absence of added volatile organic compounds (VOCs) and with VOCs added to represent urban emissions from a representative African megacity. In this part of the manuscript, we report the chemical composition of fresh and BB aerosols photochemically aged in the presence of VOCs, which were combusted at two different temperatures and collected onto filters.

Identifying the light-absorbing chromophores and non-absorbing aerosol constituents by chemically characterizing BrC is a challenging task (Lin et al., 2015b). In this Part 2 manuscript, ultra-performance liquid chromatography (UPLC) was interfaced to both photodiode array spectrophotometry (or DAD) and high-resolution quadrupole time-of-flight mass spectrometry (HR-QTOFMS) to chemically characterize BrC chromophores at the molecular level for both fresh and aged emissions, and is compared with similar measurements for BC. This technique (i.e., UPLC/DAD-ESI-HR-QTOFMS) has previously been used for the molecular level characterization of BrC constituents in laboratory-generated SOA (Lin et al., 2015a;Lin et al., 2016;Lin et al., 2014) and in ambient aerosols and cloud water impacted by BB (Kitanovski et al., 2012b;Budisulistiorini et al., 2017;Zhang et al., 2013).

2 Experimental methods

Formatted: Normal, Indent: First line: 0"

Formatted: Font:Font color: Auto

Deleted: (Smith et al., 2019a)

In companion paper Part I, (Smith et al., 2020) we described the aerosol generation and combustion system, the smog chamber characteristics, and the aging conditions and process. A summary is provided here. For laboratory samples, BB aerosols were generated by combusting 0.5 g of biomass samples in a tube furnace (Carbolite Gero, HST120300-120SN). Smoke and gases produced from combustion were sent directly into the smog chamber via a heated (200 °C), ¼ inch corrugated stainless-steel transfer tube. The North Carolina A&T State University (NCAT) indoor smog chamber has a volume of 9.01 m^3 and is lined by FEP Teflon. Two sides of the chamber each have a bank of 32 ultraviolet (UV) lights (Sylvania, F30T8/350BL/ECO, 36"), for a total of 64 lamps, to produce photochemical reactions. For the purposes of this experiment, a clean environment is maintained by flushing the smog chamber for at least 24 hours with clean air coming from a clean air generator until negligible particle concentrations are reached.

The particle size distribution was continuously measured during the experiments. In general, it took about 15−20 minutes for the size distribution to become a Gaussian distribution. In addition, we checked the total mass concentration reported by the aerosol instrument manager software and confirmed that after 15−20 minutes of combustion the mass loading become stable. We characterized this as a well-mixed condition in the chamber. An example of the size distribution for each fuel during an experiment is given in Figure S1.

For this study, authentic fuel plants were obtained from east Africa. These samples were weighed on a calibrated analytical balance so that it would approximately yield a total aerosol loading representative of a particular scenario (urban, wildfire, etc.). We utilized previously measured emission factors (Akagi et al., 2011;Simoneit, 2002;Yokelson et al., 2013;Andreae and Merlet, 2001), such as 18.5±4.1 g PM_{10} kg^{-1} wood (dry weight) for tropical forest fuels (Akagi et al., 2011). For instance, to achieve a mass loading of 1100 μg m^{-3}, which is the mean loading found in urban/suburban residential locations (Oyem and Igbafe, 2010), 0.5 g of wood was burned in these experiments. As determined by SMPS spectra and assuming a particle density of 1 g cm^{-3}, typical peak particle concentrations were 800-900 μg m^{-3} for combustion at 500 °C and ~80 μg m^{-3} for combustion at 800 °C. Since aerosol densities are generally larger than 1 g cm^{-3}, our estimated mass represents the lower limit of the actual values.

Optical measurements were performed after the chamber was mixed, since they could not be taken directly from the furnace, given the long measurement time and high particle concentrations. While several types of aging were performed in Part 1, the work presented here focuses on photochemical aging with anthropogenic VOCs, specifically benzene, toluene, and xylene. No other atmospherically active species were added, such as HONO, NOx, O_3, etc., aside from those produced during combustion or resulting from photochemical aging. VOCs were injected into the chamber just before combustion while the UV lights are turned off, followed by 12 hours of irradiation. While this is somewhat long for a chamber experiment, this length of time would represent a maximum change upon photochemical aging. Details of VOC addition is discussed in the first part of this paper (Smith et al., 2020). The purpose of adding the VOCs was to represent a polluted urban environment, where we used the emission inventory for urban environments from South Africa. This does not necessarily represent the east African emission inventory, but this serves as a baseline, since this is the only available data to us for the continent Anthropogenic VOC concentrations were based on observations from several urban sites that were in the South African Air Quality Information System (SAAQIS). Average values for mid-July, the middle of the peak burning season for South Africa

Deleted: supplementary information

Deleted:

Deleted: s detailed in Part 1, a

for the year 2016, were ~1.25, 3.5, and 1.5 ppm for benzene, toluene, and xylene, respectively. While these ratios were maintained in this chamber work, amounts introduced into the chamber were ~12 times more concentrated (15, 42, and 18 ppm, respectively) due to sample preparation constraints, since the amounts needed for an exact match were too small to weigh accurately. In previous work, the total particle volume concentration (nm^3 cm^{-3}) was found to undergo a first order decay (Smith et al., 2019). The loss rate constant for this process was $(1.34 \pm 0.02) \times 10^{-3}$ min^{-1}, which corresponds to a lifetime of 12.4 hours, so these samples underwent ~1 lifetime of particle losses. The chamber relative humidity was 0% or under the detection limit of the measurement device. Chamber temperature was 20 − 23 °C, depending on the temperature of the room. The temporal evolution of chamber temperature and other characteristics have been extensively investigated for the NCAT indoor smog chamber (Smith et al., 2019).

2.1 Fuel types and condition

Eucalyptus, Acacia, and Olive have many things in common besides their wide distribution of growth. All are Angiosperms and Eudicots. Acacia and Eucalyptus are more closely related, with both belonging to the Rosid clade, while Olive is an Astrid. This is where their evolutionary similarities end, with Acacia, Eucalyptus, and Olive in the orders Fabale, Myrtale, and Oleaceae, respectively. The common names of these species, followed by their botanical author citation are Eucalyptus (L'Hér), Acacia (Mart.), and Olive (L.). The fuel moisture content was 10%. As such, they had minimal moisture content and the fuels studied in this work are likely most relevant for situations where these fuels are combusted in home heating and cooking or as the litter component of wildfires.

2.2 Collection of filter samples

BB aerosols were collected onto 47-mm Teflon filters (Tisch Environmental, SF18040) for chemical analysis and tunneling electron microscope (TEM) grids (Ted Pella, 01844, carbon film on 400 mesh copper) for image analysis. For fresh BB aerosol, these samples were collected inline immediately after the furnace, only allowing enough distance from the furnace for the sample to cool before reaching the filters. This allowed fresh samples to be collected as close to the initial combustion as possible. Flow of the aerosol through the Teflon filter was driven by the chamber instrumentation, specifically the CO and CO_2 analyzers, at ~2.5 L min^{-1}, while flow through the TEM grid was provided by a modified aquarium pump at 0.5 L min^{-1}. With the output from the furnace at 10 L min^{-1}, pressure was maintained through the system by diverting the excess flow (7 L min^{-1}) to the exhaust. Samples were collected for the duration of the burn, which was typically around 10 minutes. In this manner, approximately 25% and 5% of the total BB aerosol were collected onto the Teflon filter and TEM grid, respectively, after losses in the tube furnace and transfer tubing.

For aged BB aerosol, samples were taken directly from the chamber. Since the aerosol had already been diluted in the chamber, a larger sample volume was necessary for deposition onto the filters. For these samples, aerosol was taken from one of the chamber outputs, with a combined flow of 5 L min^{-1} through the Teflon filter and TEM grid setup produced by a separate pump. Samples were collected for 18 min, which corresponded to 90 L of chamber

Deleted: While

Deleted: was not measured, each fuel was collected directly from the tree and allowed to dry in a fume hood for over a year

Deleted: .

Deleted: (Smith et al., 2020)

Deleted:

Formatted: Font:Font color: Auto

Deleted: 4

air, or ~1% of the total chamber volume. With aged filter samples taken after approximately 24 hours in the chamber, particle concentration had been significantly reduced since initial combustion, due to particle loss and dilution. However, the resulting samples were still large enough to be seen by the naked eye on the filter paper. Unused filters underwent the same extraction process as the sample filters to serve as a blank sample.

We estimated the approximate mass loading in the chamber during each combustion case by converting the SMPS size distribution into the total mass by assuming a density of 1 g cm^{-3}. Our estimated mass represents the lower limit of the actual values. During the 500 °C combustion cases, the typical concentration of aerosol after being well mixed was about 800 µg m^{-3}, while that of the 800 °C cases was about 100 µg m^{-3}. After 12 to 15 hours of aging, the initial mass loading was reduced by a factor of two, with a resulting concentration of about 400 µg m^{-3} and 50 µg m^{-3} during the 500 °C and 800 °C combustion cases, respectively.

Deleted: s

2.3 UPLC/DAD-ESI-HR-QTOFMS

An Agilent 1200 Series UPLC system interfaced to a 6520 Series Accurate Mass Q-TOFMS instrument (Agilent Technologies, Santa Clara, CA) and equipped with an ESI source (Lin et al., 2014) was operated in negative ion mode to chemically characterize BB organic aerosol (BBOA) constituents in filter samples collected from the tube furnace for fresh emissions and from the smog chamber for aged experiments. In brief, chromatographic separations were carried out using a Waters ACQUITY UPLC HSS T3 C_{18} column (2.1×100 mm, 1.7 µm particle size, Waters Corporation, Milford, MA) at 45 °C. The mobile phases consisted of eluent (A) 0.1% acetic acid in ultrapure water (>18 MΩ cm), and eluent (B) 0.1% acetic acid in pure methanol (99.9%, Fisher Chemical). The gradient elution program was as follows: eluent (A) held at 100% from 0 − 2 min, decreased linearly to 10% from 2−10 min, held constant at 10% between 10 −11 min, increased linearly to 100% from 11−15 min, and held constant at 100% during a 5-min post run for column re-equilibration. The sample injection volume was 5 µL at a flow rate of 0.3 mL min^{-1}. A diode array detector (DAD) between the UPLC system and the mass spectrometer was operated to measure UV-visible (UV-vis) absorbance from 200 to 800 nm with a step of 2 nm. At the beginning of each analysis period, the mass axis of the Q-TOFMS was calibrated using a commercially available ESI-L low-mass tuning mixture (Agilent Technologies, Santa Clara, CA) containing seven masses ranging from 60 -1700 Da. For real-time mass correction, a solution containing 3 reference mass components was continuously infused for real-time mass axis correction (calibration). The resultant mass resolution of the ESI-HR-QTOFMS over *m/z* 60 −1700 ranged from ~11,000 at the low mass end to ~17,000 at the high mass end. Raw data were acquired and processed with MassHunter Software (Version B.06.00, Build 6.0.633.0, Agilent Technologies, Santa Clara, CA).

2.4 Sample preparation and BrC identification

Filter samples collected as described in the last section were extracted individually in 22 mL of pure methanol by sonication for 45 minutes, blown dry under a gentle nitrogen stream at room temperature (21−22°C), and reconstituted in 300 µL of 50:50 (v/v) methanol/water solvent mixture for the subsequent UPLC/DAD-ESI-HR-QTOFMS analysis. While the water-soluble fraction of BrC is less than 70%, almost 90% of BrC can be extracted by organic solvents, such as methanol. Furthermore, the water-insoluble fraction of BrC is more absorbing than the water-

soluble fraction (Lin et al., 2017;Bergstrom et al., 2007;Laskin et al., 2018). Immediately prior to analysis, each reconstituted extract was filtered through a PTFE syringe filter (Agilent, 0.2-µm pore size) to remove undissolved particles such as soot components. A similar procedure was used by other research studies (Kumar et al., 2018;Jiang et al., 2019).

Previous work went into quantifying BrC aerosol constituents identified by UPLC/DAD-ESI-HR-QTOFMS, seven external (2-nitrophenol, 4-nitro-1-naphthol, 4-methyl-5-nitrocatechol, vanillin, vanillic acid, coniferaldehyde, and benzoic acid) commercially-available authentic standards were prepared for 6-point calibration curves from 0.004 −10 µg mL^{-1}, with detection limits below 0.004 µg mL^{-1}. While several of these methods were done in this work, determining the absolute quantity of a BrC constituent was not pursued. From the previous tests of quality control, the recovery rate of ketopinic acid was ~90% among 20 BB aerosol samples with the same extraction process with methanol and the UPLC/DAD-ESI-HR-QTOFMS method. Two filter samples (with the collected $PM_{2.5}$ masses > 1 mg) were re-extracted using 70:30 (v/v) acetonitrile/toluene solvent mixture. Most of the identified BrC species were below detection limit from this second extraction, suggesting excellent extraction efficiency for the first time with methanol. Only a few BrC aerosol constituents (e.g., vanillic acid, coniferaldehyde) were detected from the second extraction, but their abundance was lower than 1.5% of that from the first extraction. The only exception was 2-nitrophenol, whose extraction efficiency using methanol was ~55% for the first time.

Deleted:

Deleted: yl

Deleted: yl

2.5. Non-targeted analysis

Non-targeted MS analyses were performed to compare the filter samples collected from the smog chamber experiments under different conditions, such as fuel type, combustion temperature, and aging, to reveal the major molecular secondary BBOA products, with a focus on BrC. The raw data files acquired from UPLC/ESI-HR-QTOFMS were first transformed into ".mzData" format by Agilent MassHunter and then processed by the online metabolomics platform XCMS (https://xcmsonline.scripps.edu/) (Tautenhahn et al., 2012). During this transformation, only peaks that had intensities above 0.6% of the base peak were selected. Workflow parameters were adopted from previous work with modifications (Tian et al., 2017). In brief, the "centWave" algorithm was used for peak detection, with a peak width range from 5 − 60 seconds, and the mass error tolerance was set at 20 ppm. Peak alignment required an *m/z* width (mzwid) at 0.025. Generally, around 30 major BBOA constituents were filtered out by XCMS, and were then examined in MassHunter to make sure they possessed good peak shapes and were not present in the filter blank samples. The resulting blank and sample chromatograms are presented in Figure S2.

Comment [d2]: The original wording is correct, according to APA Style 6th edition. The acronym "m/z" is pronounced "em-zee", which starts with a vowel sound, and therefore is preceded by "an" instead of "a".

Deleted: the supplementary information

The following data fields were used for each compound returned by the XCMS platform: median *m/z* ratio, median retention time (rt), and the intensities for each sample in the pairwise comparison. Compounds with a similar *m/z* ratio, regardless of observed retention times had their relative intensities combined, as they most likely returned the same chemical formula. Later, for relatively large peaks with slightly different median *m/z* values, when species were found to have the same molecular formula, as determined by MassHunter (see below), their ion intensities were also combined. The amount of aerosol varies significantly from sample to sample, especially between fresh filter samples collected directly from the furnace during combustion and aged filter samples collected from the chamber, with the former always being much greater. Due to the lack of authentic standards for quantifying individual BBOA,

these masses were not determined at the time of their collection, and their spectral intensities could not be normalized to a specific aerosol mass or tracer for aerosol mass. As such, no direct comparison between samples could be made without first normalizing spectra. We normalized the intensity data by generating a scaled intensity difference between the samples using the following equation:

$$\frac{x_1}{\sum x_{1,i}} - \frac{x_2}{\sum x_{2,i}} \quad (1)$$

where x_1 is the intensity from the first sample and x_2 is the intensity from the second sample, and each term represents the fractional integrated ion intensity of their respective samples. Positive values indicate that a compound was more abundant in the first sample, while negative values indicate that a compound was more abundant in the second sample. The results of the XCMS platform were then sorted to exclude any absolute scaled intensity differences less than 0.5 %, which left around 30 compounds or fewer to identify for each pairwise comparison.

The MassHunter software was then used to confirm and identify the compounds found by the XCMS platform. For each pairwise comparison, extracted-ion chromatograms (EICs) were generated for both samples and any relevant blank samples for each of the *m/z* ratios found by XCMS. MS results were then generated from any peaks found in the EICs. MassHunter's built-in formula generator was used to identify the most likely compounds associated with the *m/z* ratio and retention time identified by XCMS. These chemical formulas, along with their double bond equivalent (DBE), mass difference, and number of chromatographic peaks (at different retention times, most likely isomers of the compound) were cataloged, with updated *m/z* ratios and retention times, as identified by MassHunter. Lastly, suggested identities were assigned to each chemical formula based on relevant literature. Any compounds that were also found in the blank sample(s) were removed from the catalog.

2.6 UV/Visible analysis

The UV/Visible spectra in this work were not done for specific molecular species, but for all molecular species that were extracted and chromatographically/spectroscopically measured. Spectra were derived by integrating across the entire chromatogram within MassHunter. Each was background subtracted from a blank run, though the resulting spectra could not be compared directly because of the reasons mentioned earlier. Since some negative absorption values were produced after background subtraction, baseline values were shifted such that the smallest absorption intensity above 250 nm was made barely positive (by 0.00001 mAU) and all values were divided by the spectral maximum to produce a peak value of 1 in the 250 – 800 nm range. The reason all values were made slightly positive was that it enabled the determination of a normalized Angstrom absorption exponent (NAAE). Because the baseline was shifted to allow for a log plot, this is mathematically different than the AAE, and should only be used for comparison purposes. With a focus on the 500 − 570 nm region, the NAAE and the normalized slope vs. wavelength was determined. Heat map chromatograms of absorption vs wavelength and retention time are given in Figure S3.

3 Results and discussion

3.1 MS analysis of fresh emissions

Because the chemical measurements of the BB aerosols derived from Acacia and Eucalyptus fuels were the most robustly sampled in this work, a comparison of those results is presented here, though a few references to Olive will be made. Figure 1 shows the UPLC/ESI-HR-QTOFMS negative ion mode difference spectra produced for these BB aerosol types. Peaks that are positive are more abundant in the Acacia-derived BB aerosol sample, while negative peaks are more present in the Eucalyptus-derived BB aerosol sample. Table 1 highlights the molecular differences between the BB aerosols derived from freshly combusted Acacia and Eucalyptus fuels, showing the scaled intensity difference for species with an absolute difference greater than 0.5 %, the mean peak *m/z*, the mass difference between the measured and the monoisotopic mass of the formula determined using MassHunter (listed here as a measure of formula identification quality), the determined formula, the double bond equivalence (DBE) of the formula, the number of chromatographic peaks seen from an EIC, and the suggested identity based on the formula and relevant literature.

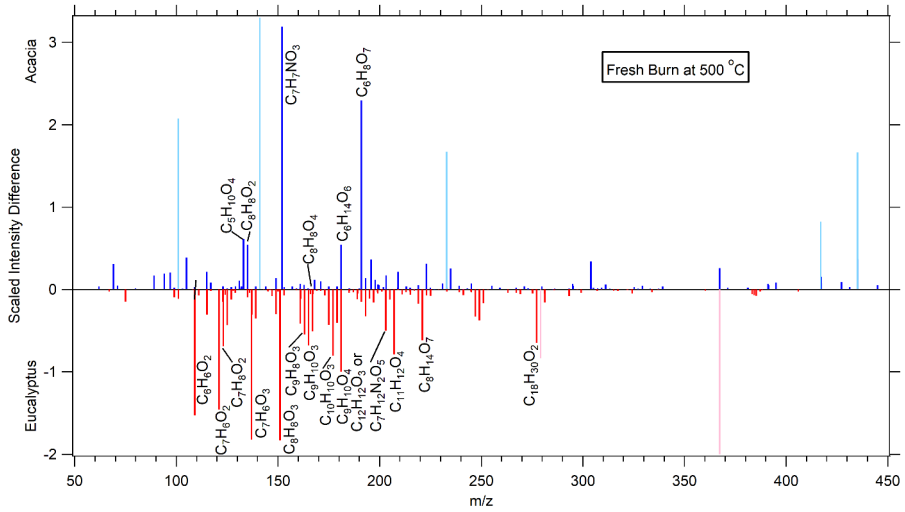

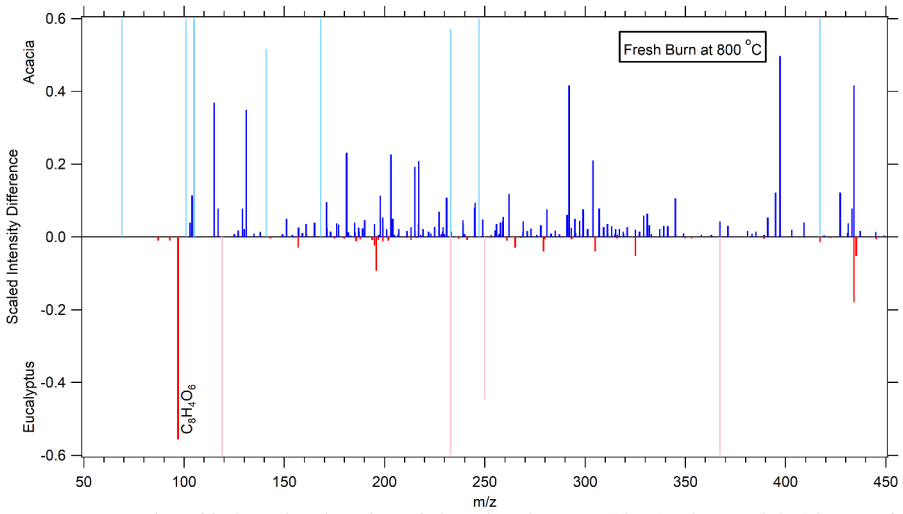

Figure 1. A comparison of fresh Acacia and Eucalyptus fuels combusted at 500 °C (above) and 800 °C (below) in terms of the scaled intensity difference (see section 2.5). Species more present in Acacia-derived BB aerosols have positive values (blue lines), while those more present in Eucalyptus-derived BB aerosols have negative values (red lines). Peaks in lighter colors were present in the XCMS analysis but were found to be present in significant amounts in the blank sample. Many of these peaks that were found in the blank extend past the scale of the plot but were cut off to focus on species associated with BB aerosol. Compounds having an absolute difference greater than 0.5% have been labeled. Far more differences are revealed at the lower temperature burn and different classes of compounds are expressed in different relative amounts for Acacia and Eucalyptus combustion.

Table 1. Molecular differences between fresh Acacia- and Eucalyptus-derived BB aerosols emitted by combustion at 500 °C (upper section) and 800 °C (lower section), measured by negative ion mode UPLC/ESI-HR-QTOFMS analysis. Species are ordered in terms of increasing scaled intensity difference, with positive values associated with Acacia-derived BB aerosols and negative values associated with Eucalyptus-derived aerosols. The mass difference is calculated as the difference between the observed median mass and the monoisotopic peak (typically singly deprotonated) of the formula determined using MassHunter. Peak counts labeled 'M' have multiple indistinct peaks, while those labeled 'W' elute over a very long retention time (1−4 minutes), both of which could easily consist of several isomers. Suggested species marked with an asterisk can, and likely do, have multiple isomers present. Those marked with a 't' are tentative assignments. Identities marked with a dagger (†) have been confirmed against an authentic standard. See the supplemental information tables for associated retention times, wherein retention times in bold are associated with an authentic standard.

	Scaled Intensity Difference	*m/z*	Mass Difference (ppm)	Formula	DBE	# of Peaks	Suggested Identity
500 °C	-1.831%	151.0403	-0.95	$C_8H_8O_3$	5	5	vanillin,[‡] and methoxybenzoic acid * or hydroxyanisaldehyde*
	-1.822%	137.02442	0.72	$C_7H_6O_3$	5	4-5	salicylic acid* or dihydroxybenzaldehyde*
	-1.526%	109.02969	-3.37	$C_6H_6O_2$	4	1	dihydroxybenzene
	-1.459%	121.02951	-0.59	$C_7H_6O_2$	5	3	benzoic acid[‡] and hydroxybenzaldehyde*
	-0.998%	181.05101	0.3	$C_9H_{10}O_4$	5	3	homovanillic acid*, dimethoxybenzoic acid*, or syringaldehyde*
	-0.801%	177.05542	1.16	$C_{10}H_{10}O_3$	6	1	coniferaldehyde[‡]
	-0.790%	207.06602	1.5	$C_{11}H_{12}O_4$	6	1	sinapaldehyde
	-0.691%	123.04541	-0.81	$C_7H_8O_2$	4	2	guaiacol*
	-0.677%	165.05548	5	$C_9H_{10}O_3$	5	M	hydroxy-methoxyacetophenone* (apocynin, paeonol, etc), caffeyl alcohol*, veratraldehyde,* or phloretic acid*
	-0.647%	277.21747	-1.11	$C_{18}H_{30}O_2$	4	1	octadecatrienoic acid (likely linolenic acid)
	-0.616%	221.06665	0.61	$C_8H_{14}O_7$	2	1-2	dihydroxydimethoxyoxane-2-carboxylic acid*[t]
	-0.545%	163.0399	nc	$C_9H_8O_3$	6	8+	caffeic aldehyde,* coumaric acids*
	-0.510%	167.03508	-0.03	$C_8H_8O_4$	5	3+	vanillic acid*[‡]
	-0.499%	203.07032	-10 - 10	$C_{12}H_{12}O_3$ or $C_7H_{12}N_2O_5$	7 or 2	W	dimethylmethoxycoumarin* or glycyl-glutamic acid[t]
	0.543%	135.04513	-2.25	$C_8H_8O_2$	5	2	anisaldehyde*, acetophenone, methylsalicylaldehyde*, or methylbenzoic acid*
	0.545%	181.07191	-1.1	$C_6H_{14}O_6$	0	4	mannitol, sorbitol, or galactitol
	0.612%	133.05005	3.92	$C_5H_{10}O_4$	1	1	deoxyribose or monoacetalglycerol[t]
	0.994%	666.05964	-	-	-	1	too many options
	2.293%	191.0198	-2.5	$C_6H_8O_7$	3	W	citric acid
	3.190%	152.03565	-4.2	$C_7H_7NO_3$	5	1	nitroanisole*, nitrocresol, or nitrobenzyl alcohol*
800 °C	-0.556%	96.960662	9	$C_8H_4O_6$	7	1	dihydroxyphthalic acid
	0.497%	397.27546	-	-	-	1	too many options
	0.560%	666.05967	-	-	-	1	too many options
	0.789%	982.993	-	-	-	W	no formula found

Except for dihydroxyphthalic acid and other tentatively assigned compounds, there is very little difference between the two fuel types when they are combusted at 800 °C. This is consistent with previous work, where flaming combustion leads to formation of predominantly BC aerosol (Reid et al., 2005). The modified combustion efficiencies (MCE), discussed in companion paper (Part I), were 0.974 ± 0.015 when averaged from 12 different burns performed at 800 °C, which supports that these aerosols represent particles that were emitted during the flaming stage of combustion, which is dominated by BC aerosol. Since most of the chemical differences between samples are very small, this suggests that either very few BrC species are produced for either fuel, or there are numerous species that are essentially the same between the samples. In Part I, Eucalyptus was shown to have a higher SSA, ~0.43 for 300 nm particles, than Acacia, which is more absorbing and has an SSA of ~0.3 at that size (see Figures 3 and 4 of Part I).

Deleted: *

Deleted: or

Deleted: or

Deleted:

Deleted:

Comment [d3]: The original wording is correct, according to APA Style 6th edition. The acronym "SSA" is pronounced "ess-ess-ay", which starts with a vowel sound, and therefore is preceded by "an" instead of "a".

This would suggest that Eucalyptus has more non-absorbing OA, or at least less absorbing than BC. It is unlikely that dihydroxyphthalic acid would produce a significant, but wavelength dependent, absorption in the 500−570 nm region of the spectrum. Conversely, it is Acacia that appears to have many more low-abundant organic constituents. This suggests one or more of the following: 1) that Eucalyptus has significantly more complex combustion products than Acacia, such that their abundances fall below the lower threshold of XCMS analysis; 2) that Eucalyptus combustion products are either unresponsive in the negative ion mode of the UPLC/ESI-HR-QTOFMS analysis, such as having very high molecular weights (MWs), which prevents them from eluting off the UPLC column, or having no acidic functionalities; 3) that those products are not extractable by methanol; 4) that those products are semi-volatile and were removed during the offline sample processing for UPLC/DAD-ESI-HR-QTOFMS analyses; or 5) that differences between the observed SSA values are due to morphology differences. Very high MW compounds, such as PAHs, are potentially present, but it is unlikely that such large molecules would lack the ability to absorb light (see Section 3.3) to produce a more scattering aerosol for Eucalyptus, thus discounting part of reason 2. Negative ion mode ESI is known to bias detection in favor of acidic compounds, such as those with carboxylic acids, nitroaromatics, sulfated organics, and those that have sufficiently acidic -OH groups. Given that light-absorbing OA seems significantly soluble in methanol (Kumar et al., 2018), reason 3 is also unlikely. If one assumes that XCMS is capturing the complexity of molecular species, it is likely that Eucalyptus products are low MW species that are semi-volatile, that those low MW species are not captured by UPLC/DAD-ESI-HR-QTOFMS analyses, that the observed differences in SSA are due to morphology differences, or a combination of the three. One potential explanation would be a compound such as eucalyptol (1,8-cineole), which is a large fraction of Eucalyptus oil, that is a cyclic ether that lacks any basic functionality, has good solubility in alcohols, and does not absorb in the UV and visible. When extracting essential oil from Eucalyptus leaves by water-steam distillation, an oil yield of 0.3 – 2.0% (dry wt.) was produced of which 7 – 75% was eucalyptol, depending on the species (Masamba et al., 2001;Subramanian et al., 2012). The presence of such a compound should be apparent under positive ion mode ESI or atmospheric pressure chemical ionization MS analysis and possibly FT-IR if present in sufficient quantities.

Combustion of each fuel at 500 °C presents a very different picture, not only because of the number of species differentiated by their mass, but also the number of isomers present for each mass. The number of chromatographic peaks in the EICs are listed for each mass in Table 1. In that table, all species are present in both samples to differing degrees, except for octadecatrienoic acid, which is likely linolenic acid, and is only present in Eucalyptus. Demonstrating this complexity, for instance, *m/z* 151.04 was vanillin (a hydroxy methoxy benzaldehyde confirmed with an authentic standard) (Budisulistiorini et al., 2017) and hydroxyanisaldehyde and/or methoxybenzoic acid (such as anisic acid), but consists of five isomers, likely differing in the placement of functional groups along the aromatic ring. These are previously observed lignin pyrolysis products (Simoneit, 2002) that are more prevalent in Eucalyptus. This includes only one isomer of dihydroxybenzene, which is likely catechol (Simoneit, 2002), though resorcinol is also possible, since it has been observed in gas-phase measurements of prescribed fires (Yokelson et al., 2013). At least four isomers of hydroxybenzoic acid, such as salicylic acid, and/or dihydroxybenzaldehyde, are present and more abundant in Eucalyptus. While these compounds have the same structural motifs as other lignin pyrolysis products, only salicylic acid (Fleming et al., 2019) and 4-hydroxybenzoic acid (Bi et al., 2008) have been observed previously

Deleted: h

Deleted: is likely

Deleted: /or

as BrC chromophores associated with BB, which suggests that there are at least two other unidentified isomers. Other lignin pyrolysis products are noticeably more abundant for Eucalyptus combustion at 500 °C and are likely BrC chromophores, such as benzoic acid (confirmed by an authentic standard) and two isomers of hydroxybenzaldehyde at *m/z* 121; homovanillic acid, dimethoxybenzoic acid, and/or syringaldhyde (3 isomers observed) at *m/z* 181 (Simoneit, 2002); coniferaldehyde at *m/z* 177 (confirmed); sinapaldehyde (and not another isomer) at *m/z* 207 (Fleming et al., 2019); guaiacol and some other isomer at *m/z* 123; and the ubiquitous vanillic acid at *m/z* 167 (confirmed) (Fleming et al., 2019;Simoneit, 2002). Distillation products more prevalent in Eucalyptus include an indistinct number of isomers of hydroxy-methoxyacetophenone (e.g. apocynin or paeonol), caffeyl alcohol, and/or phloretic acid at *m/z* 165. The last distillation product expressed more in Eucalyptus is at least one isomer of what is likely dimethyl methoxycoumarin. These species have been observed previously as a class of compounds (Fleming et al., 2019;Lin et al., 2016), though not this one particularly to the author's knowledge. At least eight isomers of caffeic aldehyde, veratraldehyde, and/or coumaric acid are also present.

Other species are present in greater abundance in Acacia at 500 °C. Saccharides such as mannitol and sorbitol have been observed as pyrolysis products of cellulose and in road dust (Simoneit et al., 2004), though two more isomers, one likely being galactitol ($C_6H_{14}O_6$), are also present. Similarly, citric acid has been observed as products from saccharide combustion (Bi et al., 2008), though the authors have not been able to find references to deoxyribose or monoacetalglycerol in the literature. Nitroaromatic species have been shown to be produced during the pyrolysis process from fresh combustion in this work, where one isomer of nitroanisole, nitrocresol, or nitrobenxyl alcohol is present and produced in significantly higher quantities in Acacia than Eucalyptus.

Work by Fleming et al. (2019) shows that sinapaldehyde and coniferaldehyde are two known lignin pyrolysis products that are produced from their corresponding lignin monomeric units; specifically sinapyl and coniferyl alcohol. They also state that these species are anticorrelated, where sinapaldehyde is more prevalent in angiosperms and flowering fuels, while coniferaldehyde is more abundant in conifers and soft woods. We examined our BBOA mass spectra for sinapaldehyde ($C_{11}H_{12}O_4$, $[M\text{-}H]^-$= 207.0657) and coniferaldehyde ($C_{10}H_{10}O_3$, $[M\text{-}H]^-$ = 177.0552) and found that both had a single peak with a coeluting retention time of ~9.2 minutes. Additionally, both species were found in all three fuels – Eucalyptus, Acacia, and Olive. When integrating the chromatogram between 9.0 and 9.5 minutes and extracting the resulting mass spectrum, a comparison of relative ion intensities was made. The coniferaldehyde/sinapaldehyde ratio was found to be 1.6, 3.4, and 2.6 for Eucalyptus, Acacia, and Olive, respectively. In contrast to Fleming et al. (2019), we found that all of these species (all angiosperms) had a consistently higher amount of confieraldehyde than sinapaldehyde, though this ratio varied by about a factor of 2 between species studied here. One possible reason for this was that Fleming et al. reported their results in terms of absorption intensity; not ion intensity. Since these species coeluted during our separation, it was not possible to distinguish them on that basis.

According to the above analysis, there should be more, and more varied, species present in Eucalyptus than Acacia. The main species present in greater abundances in Acacia are derived from sugars and cellulose, and are not chromophores. In Part I of this work, we found that Acacia has higher SSA than Eucalyptus when combusted at 500 °C, by 0.1 − 0.2, depending on particle size. This suggests that either Acacia has larger absolute amounts of non-chromophore compounds or Eucalyptus has a greater quantity of chromophores whose absorptive properties extend

Deleted:

Deleted:

to the 500 − 570 nm region of the visible spectrum. This will be discussed in further depth when relating MS results to UV/Visible absorption results in Section 3.3.

3.2. MS Analysis of Aging Effects

Figure 2 is similar to Figure 1, but rather than contrast different species, a single species, Eucalyptus, is differentiated in terms of the aging process. Peaks with positive values indicate those that are more present in the fresh sample, while those with negative values are more present in the aged one. Another way to interpret this is that those with positive values are no longer present in the aged sample, because they have been chemically changed due to the aging process. Those with negative values are either being produced by the aging process or are durable enough to be more significant, in a relative sense, in the aged sample. Again, we have attempted to identify compounds that change by more than 0.5 %, indicating the molecular formula for those in Figure 2, and listing them in Table 2 along with their suggested identities. Similarly, Figure 3 and Table 3 show the results for fresh versus aged Acacia.

Deleted: indicated

Deleted: ir

Deleted: listed

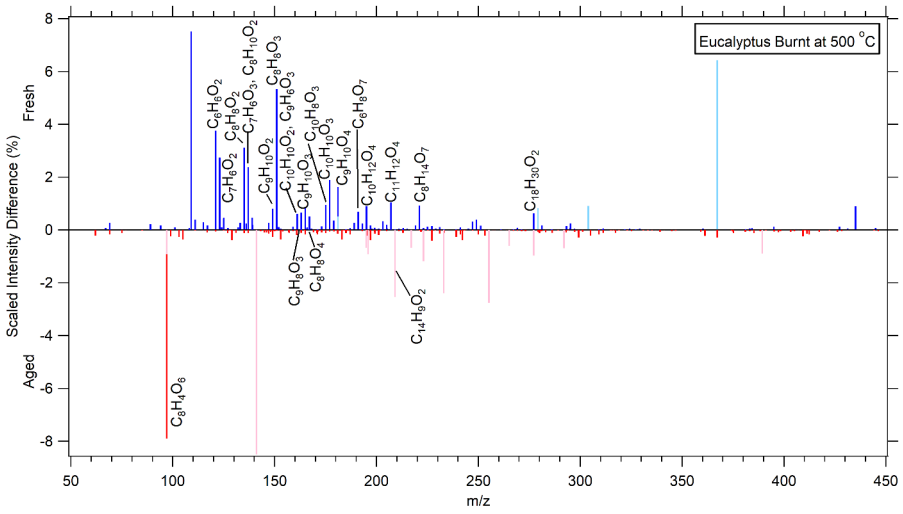

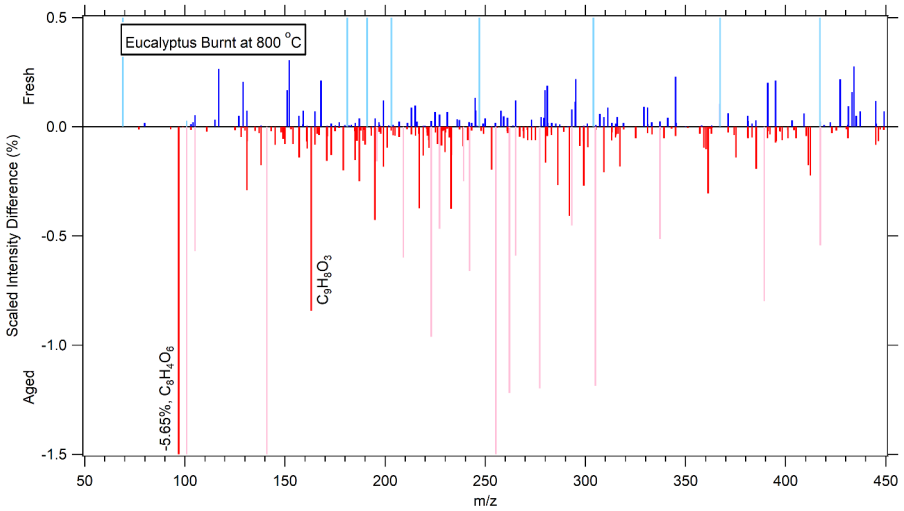

Figure 2. A comparison of Eucalyptus-derived BB aerosol combusted at 500 °C (above) and 800 °C (below) under fresh and photochemically aged conditions with VOCs in terms of the scaled intensity difference (see section 2.5). Species more present in the fresh sample have positive values (blue lines), while those more present in the aged sample have negative values (red lines) (i.e. species with positive values have been removed because of the aging process, while those with negative values are either produced or represent a greater relative contribution to the aged sample). Peaks in lighter colors were present in the XCMS analysis but were found to be present in significant amounts in the blank sample. Many of these peaks that were found in the blank extend past the scale of the plot but were cut off to focus on species associated with BB aerosol. Compounds having an absolute difference greater than 0.5% have been labeled. There is very little change for combustion at 800 °C, while 500 °C shows a net removal of many compounds.

Table 2. Molecular difference between fresh and aged Eucalyptus revealed by negative mode MS analysis. See the caption of Table 1 for more details.

	Scaled Intensity Difference	*m/z*	Mass Difference (ppm)	Formula	DBE	# of Peaks	Suggested Identity
	-8.301%	666.05954	-	-	-	1	too many options
	-7.909%	96.960595	9	$C_8H_4O_6$	7	1	dihydroxyphthalic acid
	-1.292%	209.06166	-6.5	$C_{14}H_{10}O_2$	10	1	dihydroxyanthracene
	-0.546%	649.55411	0.06	$C_{39}H_{74}N_2O_5$	4	1	unknown, potential dinitro species
500 °C	0.501%	161.02415	-0.12	$C_9H_6O_3$	7	6+	umbelliferone or other hydroxycoumarin*
	0.504%	167.03476	-0.03	$C_8H_8O_4$	5	3+	vanillic acid[†]
	0.597%	161.06082	-0.94	$C_{10}H_{10}O_2$	6	2	methoxycannamaldehyde, methylcinnamic acid, methylhydrocoumarin
	0.618%	277.21747	-1.11	$C_{18}H_{30}O_2$	4	1	octadecatrienoic acid (likely linolenic acid)
	0.641%	163.04002	-0.14	$C_9H_8O_3$	6	8+	caffeic aldehyde,* coumaric acids*

	0.686%	191.01981	-1.54 or -8.07	$C_7H_4N_4O_3$ or $C_6H_8O_7$	8 or 3	4-5	unknown; citric acid
	0.796%	149.06075	-0.03	$C_9H_{10}O_2$	5	4-5	acetylanisole,* hydrocinnamic acid,* tolylacetic acid
	0.814%	165.0556	-0.14	$C_9H_{10}O_3$	5	M	hydroxy-methoxyacetophenone* (apocynin, paeonol, etc), caffeyl alcohol,* veratraldehyde,* phloretic acid*
	0.865%	137.06088	0.98	$C_8H_{10}O_2$	4	2	anisyl alcohol, creosol, dimethoxybenzene*
	0.891%	195.06638	-0.15	$C_{10}H_{12}O_4$	5	2	acetosyringone*, homoveratic acid*
	0.919%	221.06627	0.61	$C_8H_{14}O_7$	2	1-2	dihydroxydimethoxyoxane-2-carboxylic acid*[t]
	0.942%	175.0402	0.03	$C_{10}H_8O_3$	7	7	methoxycoumarin,* methylhydroxycoumarin*
	1.030%	207.06603	1.5	$C_{11}H_{12}O_4$	6	1	sinapaldehyde
	1.621%	181.05061	0.3	$C_9H_{10}O_4$	5	3	homovanillic acid*, dimethoxybenzoic acid or syringaldehyde*
	1.888%	177.05541	1.16	$C_{10}H_{10}O_3$	6	1	coniferaldehyde[‡]
	2.371%	137.02443	0.72	$C_7H_6O_3$	5	4-5	salicylic acid* or dihydroxybenzaldehyde*
	2.737%	123.04531	-0.81	$C_7H_8O_2$	4	2	guaiacol
	3.107%	135.0451	-2.25 - 0.05	$C_8H_8O_2$	5	5	anisaldehyde,*methylbenzoic acid*, acetophenone, or methylsalicylaldehyde*
	3.746%	121.02951	-0.59	$C_7H_6O_2$	5	3	benzoic acid[†] and hydroxybenzaldehyde*
	5.335%	151.04027	-0.95	$C_8H_8O_3$	5	5	vanillin,[‡] and methoxybenzoic acid,* or hydroxyanisaldehyde*
	7.514%	109.02957	-3.37	$C_6H_6O_2$	4	1	dihydroybenzene
800 °C	-5.654%	96.961	9	$C_8H_4O_6$	7	1	dihydroxyphthalic acid
	-1.247%	649.55378	-2.61	$C_{39}H_{74}N_2O_5$	4	W	unknown, potential dinitro species
	-0.844%	163.040	-0.14	$C_9H_8O_3$	6	8+	caffeic aldehyde,* coumaric acids*
	0.856%	666.060	-	-	-	1	too many options
	1.237%	982.99221	-	-	-	W	no formula found

Deleted: dimethoxycinnamic acid

Deleted:

Deleted: , salicylaldehyde

Deleted: *

At 800 °C, there appears to be very little occurring due to the aging process in the presence of UV light and VOCs. This suggests that there were very few BrC species to begin with and that the presence of anthropogenic VOCs did not significantly impact the chemical makeup of these aerosols. It is also possible that semivolatile species produced during oxidation of these VOCs were lost in significant quantities to the chamber walls rather than the particle phase. The only significant products of oxidation were dihydroxyphthalic acid, which is likely a product of xylene oxidation, and a mixture of caffeic aldehyde, veratraldehyde, and/or hydroxy cinnamic acid isomers, such as coumaric acid. Examining the SSA changes due to aging under either dark or UV illuminated conditions was not possible for the experimental reasons stated in Part I.

Eucalyptus combusted at 500 °C is far more complex. Since many of these compounds have been discussed in more depth earlier, this discussion will only focus on compounds that are distinctly different as a function of age or those not previously mentioned. Another distillation product, benzoic acid and the lignin pyrolysis product hydroxybenzaldehyde isomer (such as salicylaldehyde), likely underwent similar processing. Derivatives of the aromatic lactone coumarin are also known distillation products present in biomass burning (Fleming et al., 2019;Laskin et al., 2015). While not as prevalent as lignin pyrolysis products, a significant number do seem to be consumed due to UV irradiation and/or photochemistry. This includes species that were not distinctly different from

Deleted: /or

Acacia, as discussed earlier, such as seven isomers of methoxy- and/or methylhydroxycoumarin ($C_{10}H_8O_3$, $[M\text{-}H]^-$ = 175.0402), neither of which have been previously observed to the author's knowledge. Others include all six possible isomers of hydroxycoumarin ($C_9H_6O_3$, $[M\text{-}H]^-$ = 161.0241), of which umbelliferone has been previously observed (Fleming et al., 2019). There are also multiple indistinct peaks that can correspond to one of several hydroxy methoxyacetophenones (apocynin (acetovanillone), paeonol, etc.), caffeyl alchohol, and/or phloretic acid ($C_9H_{10}O_3$, $[M\text{-}H]^-$ = 165.0556), many of which have been extracted from various plants but have not been observed as constituents of BBOA. There are 4 – 5 isomers of acetylanisole or, less likely, hydrocinnamic acid or tolyacetic acid. Octadecatrienoic acid has also been removed, likely by a reaction of one of its double bonds with ozone or OH radical.

In comparison, the compounds being removed from Eucalyptus combusted at 500 °C is dominated by lignin pyrolysis products. Most of these have already been discussed earlier. One isomer of dihydroxybenzene, being either resorcinol or catechol, was a pyrolysis product, and seems sensitive to the aging process, such as oxidation by OH or by bleaching, since it absorbs in the UV at 290 nm (Dewar et al., 1958). Both proper isomers of acetosyringone and/or homoveratic acid ($C_{10}H_{12}O_4$, $[M\text{-}H]^-$ = 195.0664), have previously been observed (Simoneit, 2002) and may be present here, though it cannot be definitively stated that these specific isomers are present. Highlighting the smoldering conditions present during combustion at this temperature, there are two isomers of either anisyl alcohol, creosol, or some dimethoxybenzene compound ($C_8H_{10}O_2$, $[M\text{-}H]^-$ = 137.0609). These are thought to be precursors of other, more highly oxygenated pyrolysis products of lignin, such as anisic acid, vanillin, or vanillic acid (Simoneit, 2002). These have similar structural motifs as lignin products and they may be regarded as distillation products. There are only a few compounds produced because of aging, such as dihydroxyphthalic acid and a very high MW compound identified as $C_{39}H_{74}N_2O_5$, which may be a dinitro compound. As mentioned previously, dihydroxyphthalic acid could be a product of xylene oxidation, but no enhancement of OA was observed in Part I of this work when comparing aging under lights to lights with anthropogenic VOCs. While there is a slight increase in SSA due to the presence of VOCs, it would be difficult to point to this one compound as the sole difference. Lastly, there is dihydroxyanthracene, which is likely a secondary oxidation product of the PAH anthracene. This compound should absorb in the UV and visible, given the absorption of 1-hydroxyanthracene from the UV to ~410 nm (Tichy, 1967).

Figure 3 and Table 3 show the results from aged Acacia. As before, very little has changed for the Acacia fuel combusted at 800 °C. Combustion at 500 °C is far richer and consists almost exclusively of compounds that have been consumed (i.e. have a positive scaled intensity difference). The species undergoing the most significant loss is either resorcinol or catechol. The second most consumed compound, which was not seen previously, is one isomer that is either nitroanisole, nitrocresol, or possibly nitrobenzyl alcohol ($C_7H_7NO_3$, $[M\text{-}H]^-$ = 152.0356). Given that it is being consumed over the course of the aging process, it was likely formed as a primary species during combustion of lignin in the presence of NO_x. While this species has not been observed previously, related compounds such as nitrocatechol and methyl nitrocatechol have (Fleming et al., 2019). Given that these compounds have absorption spectra that extend to ~500 nm, they were likely decomposed due to photo-bleaching, though heterogeneous reactions with OH cannot be ruled out. It is likely that the products of this photo-bleaching and/or oxidation were numerous, and each had an abundance that was too small to be captured in this analysis.

Deleted: to

Deleted:

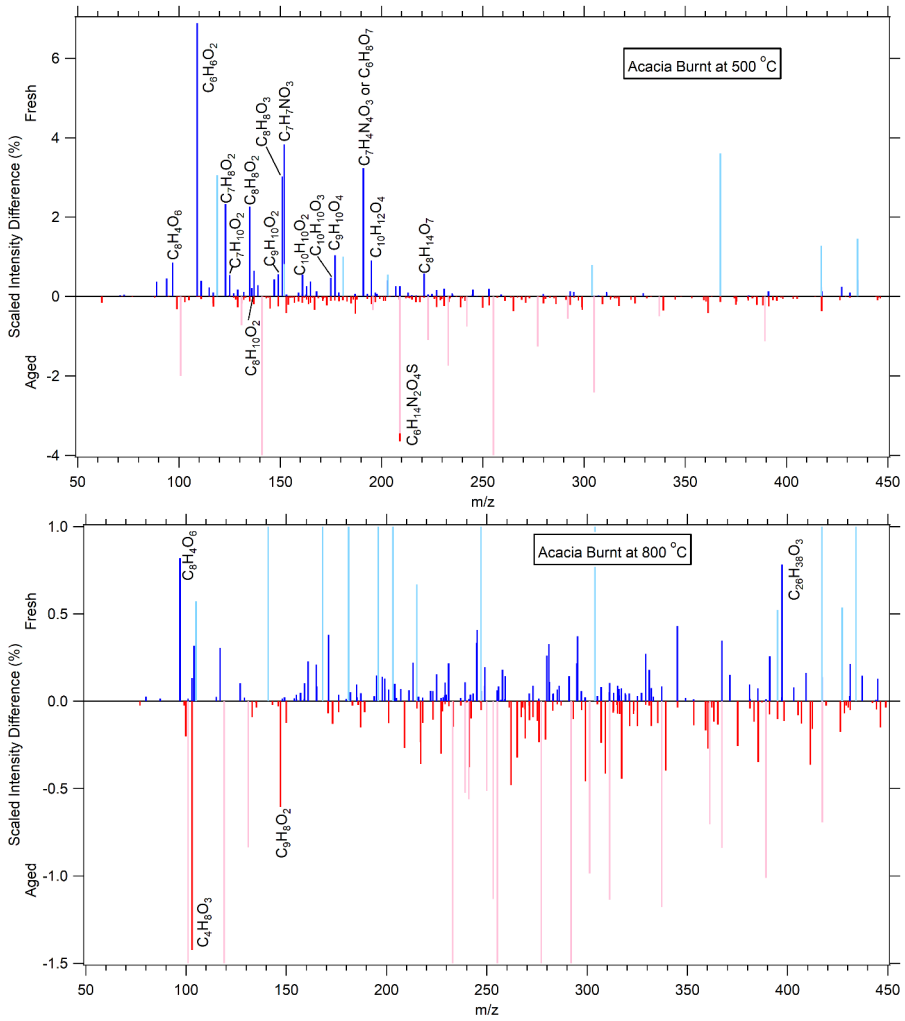

Figure 3. A comparison of Acacia-derived BB aerosol combusted at 500 °C (above) and 800 °C (below) under fresh and photochemically aged conditions with VOCs in terms of the scaled intensity difference (see section 2.5). Species more present in the fresh sample have positive values (blue lines), while those more present in the aged sample have negative values (red lines) (i.e. species with positive values have been removed because of the aging process, while those with negative values are either produced or represent a greater relative contribution to the aged sample). Peaks in lighter colors were present in the XCMS analysis but were found to be present in significant amounts in the blank sample. Many of these peaks that were found in the blank extend past the scale of the plot but were cut off to focus on species associated with BB aerosol. Compounds having an absolute difference

greater than 0.5% have been labeled. There is very little change for combustion at 800 °C, while 500 °C shows a net removal of many compounds.

Table 3. Molecular difference between fresh and aged Acacia revealed by negative mode MS analysis. See the caption of Table 1 for more details.

	Scaled Intensity Difference	*m/z*	Mass Difference (ppm)	Formula	DBE	# of Peaks	Suggested Identity
500 °C	-3.652%	209.06134	-7.41	$C_6H_{14}N_2O_4S$	1	1	unknown
	0.521%	736.13744	-0.53	$C_{44}H_{23}N_3O_9$	35	1	unknown
	0.539%	125.06093	-3.35	$C_7H_{10}O_2$	3	1	cyclohexene carboxylic or heptadienoic acid
	0.549%	161.0607	-0.94	$C_{10}H_{10}O_2$	6	2	methoxycannamaldehyde, methylcinnamic acid, or methylhydrocoumarin
	0.557%	149.06125	-0.03	$C_9H_{10}O_2$	5	4-5	acetylanisole*, hydrocinnamic acid*, tolylacetic acid
	0.575%	221.06668	0.61	$C_8H_{14}O_7$	2	1-2	dihydroxydimethoxyoxane-2-carboxylic acid*[t]
	0.641%	137.06111	-4.02	$C_8H_{10}O_2$	4	2	anisyl alcohol, creosol, dimethoxybenzene*
	0.763%	181.05141	0.3	$C_9H_{10}O_4$	5	3	homovanillic acid*, dimethoxybenzoic acid*, or syringaldehyde*
	0.852%	96.960701	9	$C_8H_4O_6$	7	1	dihydroxyphthalic acid*
	0.901%	195.06627	-0.15	$C_{10}H_{12}O_4$	5	2	acetosyringone* or homoveratic acid*
	1.038%	177.05542	1.16	$C_{10}H_{10}O_3$	6	1	coniferaldehyde[‡]
	1.306%	666.05965	-	-	-	1	too many options
	2.259%	135.04538	-2.25	$C_8H_8O_2$	5	2	anisaldehyde*, acetophenone, methylsalicylaldehyde*, or methylbenzoic acid*
	2.327%	123.04542	-0.81	$C_7H_8O_2$	4	2	guaiacol
	3.016%	151.04032	-0.95	$C_8H_8O_3$	5	5	vanillin[‡] and methoxybenzoic acid* or hydroxyanisaldehyde*
	3.233%	191.01941	-1.54 or -8.07	$C_7H_4N_4O_3$ or $C_6H_8O_7$	8 or 3	4-5	unknown; citric acid
	3.821%	152.03561	4.2	$C_7H_7NO_3$	5	1	nitroanisole*, nitrocresol*, or nitrobenzyl alcohol*
	6.886%	109.02984	-3.37	$C_6H_6O_2$	4	1	dihydroxybenzene
800 °C	-1.423%	103.02421	-4.1	$C_4H_8O_3$	1		hydroxybutanoic acid, methoxypropanoic acid
	-0.604%	147.04672	-8.72	$C_9H_8O_2$	6	W	cinnamic acid
	0.783%	397.26686	-0.08	$C_{26}H_{38}O_3$	8	1	uncertain
	0.819%	96.960676	nc	$C_8H_4O_6$	7		dihydroxyphthalic acid*
	3.467%	666.05938	-	-	-	1	too many options

Given that one isomer of dihydroxybenzene undergoes the greatest change upon aging, it is worth examining potential chemical transformations further. While resorcinol is a potential identity, catechol has gained significant attention due to its involvement as a precursor to a strong chromatophore. Catechol can react in the atmosphere to

Deleted: U
Deleted: or
Deleted: or
Deleted:
Deleted: ate
Deleted: *,
Deleted: ,
Deleted:
Deleted: dihydroxyphthalate

form 4-nitrocatechol ($C_6H_5NO_4$) through photochemical and dark processes in the gas and aqueous phase through a number of mechanisms (Finewax et al., 2018;Kroflič et al., 2018;Vidovic et al., 2018;Wang et al., 2019). Given the dryness of our chamber and the presence of UV irradiation, this mechanism would proceed through hydrogen abstraction from the hydroxyl by OH to produce a *β*-hydroxyphenoxy/*o*-semiquinone radical, followed by radical-radical combination with NO_2 (Finewax et al., 2018). Both fresh and aged spectra for 500 °C combustion were examined for nitrocatechol ($(M-H)^-$ at *m/z* 154.0140), and it was found at a rt of 8.39-8.55 min in both fresh and aged Acacia and Eucalyptus. There was a greater abundance in the aged samples, despite the mass loading on the filter being lower, suggesting a small amount from primary emission, but mainly a product of secondary formation for both fuels.

Smoldering-dominated burns were also examined for other nitroaromatic species. Methyl nitrocatechol, which has been identified as a tracer for BB SOA (Iinuma et al., 2010), and nitroguaiacol both have the formula of $C_7H_7NO_4$ and would have an $(M-H)^-$ peak at *m/z* 168.0297. Fresh Eucalyptus had two peaks at retention times of 7.71 and 9.31 min, while Acacia only had a single peak at 9.30 min. Using the exact mass and the rt, this peak at 9.30 min has been identified as 4-methyl-5-nitrocatechol, so the 7.71 min peak must be another isomer produced in fresh combustion. Since this compound must be more polar to elute earlier, it may be the 4-, 5-, or 6- isomer of nitroguaiacol (Bluvshtein et al., 2017;Kitanovski et al., 2012a). Upon aging, both fuels had two peaks with smaller absolute abundances at 9.5-9.6 and 10.0 min. The 9.5-9.6 min peak is likely a slightly shifted 4-methyl-5-nitrocatechol, suggesting both a primary and secondary source of the compound. Based on previous observations of BB aerosol, the 10.0 min peak is either 3-methyl-6-nitrocatechol, 3-methyl-5-nitrocatechol, or 4-nitroguaiacol, whose sensitivity can be altered for it to elute either before or after 4-methyl-5-nitrocatechol (Bluvshtein et al., 2017;Kitanovski et al., 2012a). Nitrophenol ($C_6H_5NO_3$, $(M-H)^-$ at *m/z* 138.0191) and nitrocresol ($C_7H_7NO_3$, $(M-H)^-$ at *m/z* 152.0348) are secondary products of phenol and cresol, respectively. Neither was observed for fresh Eucalyptus and Acacia. There are at least two forms of methyl nitrophenol in aged Acacia (rt of 10.15 and 10.46 min) and only one (rt 10.47 min) in aged Eucalyptus. Several isomers have been observed in BB aerosol in previous studies, including 3-methyl-4-, 2-methyl-4-, and 2-methyl-6-nitrophenol (Bluvshtein et al., 2017;Kitanovski et al., 2012a). The peak with a rt of ~10.46 was likely a slightly shifted 4-nitro-*o*-cresol, which was a standard compound run during the analysis of fresh BB aerosol and had a rt of 10.30 min. One nitrophenol peak at 9.37 min was observed in aged Acacia, while aged Eucalyptus did not exhibit any nitrophenol. This had a different rt than the 2-nitrophenol standard, which had a rt of 10.05 min, suggesting it was some other isomer. Nitronaphthol ($C_{10}H_7NO_3$, $(M-H)^-$ at *m/z* 188.0348) was not observed in any spectra.

3.3 UV/Visible analysis of fresh versus aged emissions

In the companion paper Part I of this work, we found, as expected, that the SSA of Eucalyptus and Acacia increased after photochemical aging for 12 hours. For instance, 300 nm particles from Eucalyptus combustion at 500 °C went from an SSA of ~0.67 to almost unity, with only a slight increase due to the presence of VOCs. Acacia increased from ~0.78 to 0.90 − 0.95 after aging, with no apparent change due to VOCs. Since these measurements

Comment [d4]: The original wording is correct, according to APA Style 6th edition. The acronym "SSA" is pronounced "ess-ess-ay", which starts with a vowel sound, and therefore is preceded by "an" instead of "a".

were size selected and this increase was observed for all selected sizes, the SSA change could not be attributed to bulk changes within the aerosol, such as particle coagulation. Such an increase in SSA resulting from morphology changes alone seems implausible, so the particles themselves must become less absorbing with age. This would be because of a loss of absorbing compounds in the 500 − 570 nm region, the formation of non-absorbing SOA that alters the real portion of the refractive index, or both. In this section, we discuss how these changes in molecular composition affect the integrated UV/Visible absorption spectrum and how these relate to the SSA of *in situ* aerosol studied in Part I of this work.

Schuster et al. (2016) found a strong correlation between AAE and the spectral variability of the refractive index of BB aerosols ($\kappa_{440}/\kappa_{700}$), with a linear correlation of $R \geq 0.939$. BrC is spectrally dependent, with a greater imaginary part of the refractive index at 440 nm (κ_{440}) than the red region of the spectrum (κ_{700}). Figure 4a shows that UV absorption dominates for fresh BB aerosol combusted at 500 °C, with a negative slope in the 500 − 570 nm range, indicating the presence of BrC can alter the absorption in the mid-visible region. This is corroborated by large *in situ* values of AAE ($\gtrsim 1.5$) for these samples as seen in Table 4. BC, on the other hand, is spectrally independent ($\kappa_{440}/\kappa_{700} \approx 1$), and has AAE values between 0.5 and 1.5, as seen for the CRDS measurements in Table 4. This is corroborated by Figure 4b and Table 4, which shows that absorption in this range has a slope of zero within the measurement uncertainty for fresh BB aerosol combusted at 800 °C; all within 1σ, except Olive, which is within 2σ. The NAAE values based on UV/Vis measurements of molecular chromophores do not conform to this trend at 800 °C; however, this is likely because they have been normalized. Lastly, AAE can reach negative values when absorption is higher at longer wavelengths (near 700 nm). Table 4 suggests that as BB aerosols are aged in the presence of UV light, they become more absorbing at longer wavelengths (except for Eucalyptus combusted at 800 °C, as measured by CRDS). This could be caused by formation of species that absorb at such long wavelengths, such as nitro-aromatic species and functionalized PAHs, or lensing effects from hygroscopic growth (Fleming et al., 2019;Liu et al., 2017).

Deleted: i

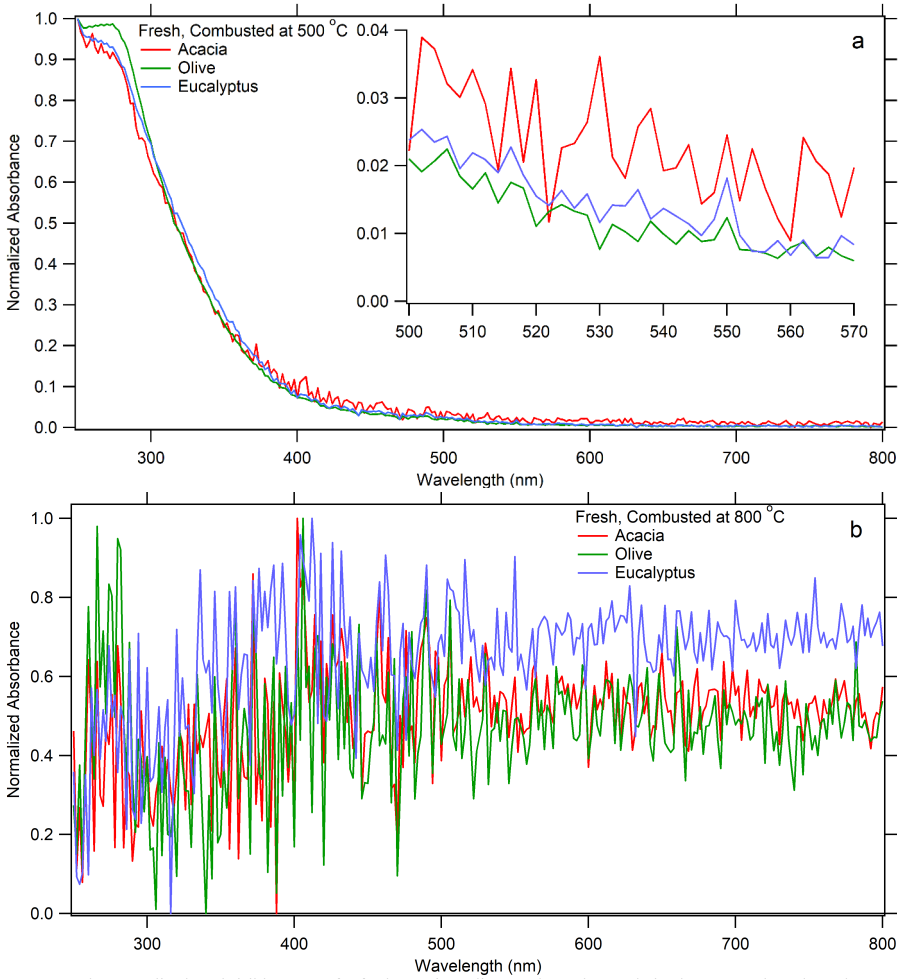

Figure 4. The normalized UV/Visible spectra for fresh Acacia-, Olive-, and Eucalyptus-derived BB aerosol combusted at 500 °C (a) and 800 °C (b). These spectra have been averaged over the entire chromatogram, background subtracted, and normalized, as described in section 2.6.

Table 4. The slope of absorption vs. wavelength and the Ångstrom absorption exponent for each sample, as measured by the UV/Vis spectrum during chemical analysis (normalized), and during CRDS/Nephelometer analysis (*in situ*). AAE was determined for the wavelength range $500\ \text{nm} \leq \lambda \leq 570\ \text{nm}$.

			AAE (normalized for UV/Vis)			Slope ($\times 10^{-5}$ nm^{-1} for UV/Vis, $\times 10^{-16}$ m^2•particle^{-1}•nm^{-1} for CRDS/Neph)		
			Acacia	Eucalyptus	Olive	Acacia	Eucalyptus	Olive
UV/Vis	500 °C	Fresh	5.55±1.21	9.53±0.72	9.10±0.64	-23.7±4.8	-24.6±1.9	-20.6±4.3
		Aged	-0.12±1.25	-1.87±1.25	-	-2.15±9.52	10.3±8.8	-
	800 °C	Fresh	0.40±0.60	0.91±0.51	0.22±0.84	-48.5±60.3	-120±69	-34.5±76.6
		Aged	-0.13±0.49	-1.88±1.01	-	4.33±70.5	145±91	-
CRDS/Neph (300 nm)	500 °C	Fresh	2.52±0.27	1.71±0.18	1.32±0.33	-1.98±0.21	-2.02±0.21	-1.63±0.412
		Aged	-3.25±0.98	-4.20±3.12	-	1.29±0.4	0.46±0.42	-
	800 °C	Fresh	0.57±0.25	0.66±0.22	0.25±0.15	-0.57±0.25	-1.64±0.53	-0.620±0.367
		Aged	-5.54±0.53	0.77±0.14	-	1.81±0.16	-2.98±0.55	-

For both Eucalyptus and Acacia combusted at 500 °C, the greatest loss of UV absorptivity, as seen in Figure 5a, happens between $260 - 350$ nm, peaking at ~290 nm. Many of the lignin pyrolysis products are consumed upon aging, due to either photo-bleaching or oxidation. Previous work has shown a reduction in BrC absorptivity due to photochemical aging (Sumlin et al., 2017) and OH oxidation (Dasari et al., 2019;Schnitzler and Abbatt, 2018). Most of these compounds absorb in the UV between 200 and 350 nm, with the notable exception of coniferaldehyde and sinapaldehyde, which both peak near $340 - 345$ nm and absorb past 400 nm (Fleming et al., 2019).

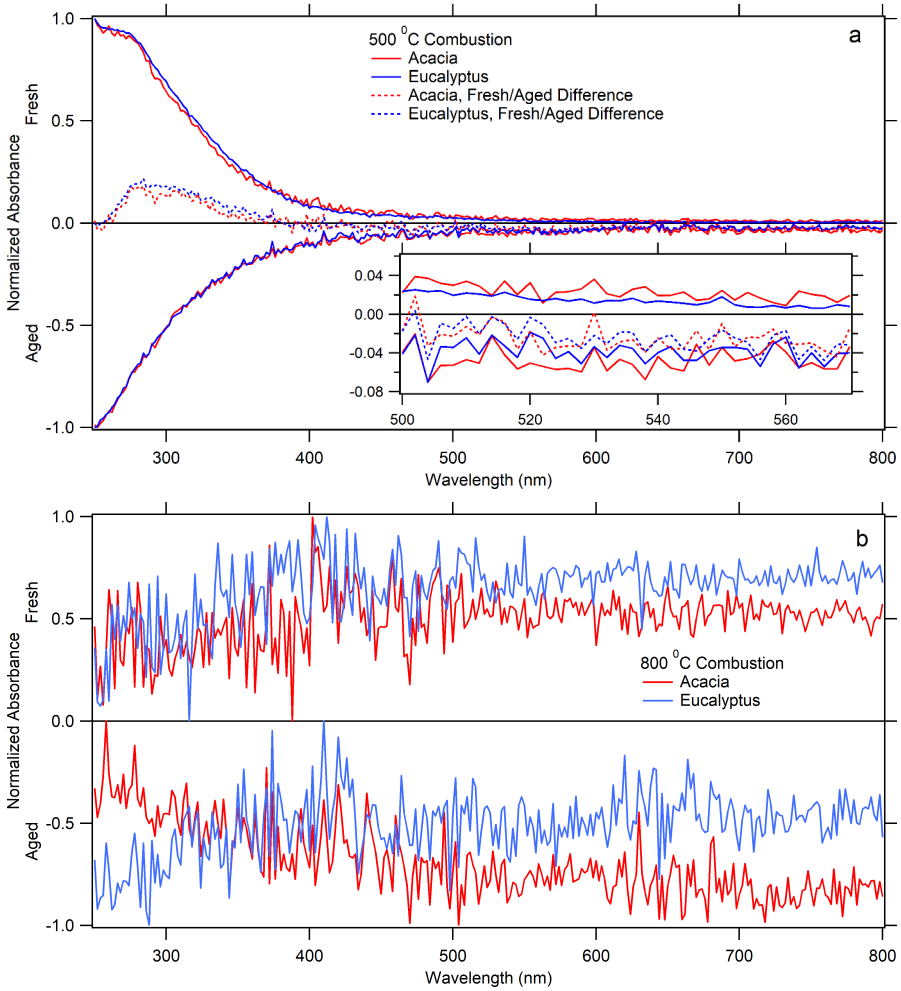

660 **Figure 5**. The UV/Visible spectrum for each fuel combusted at 500 °C (a) and 800 °C (b), showing the result from fresh combustion with positive values and photochemically aged with negative values. These spectra have been averaged over the entire chromatogram, background subtracted, and normalized, as described in section 2.6. The differences between them are highlighted with the dashed line and a blowup of the 500 − 570 nm region is presented in the inset.

665 **3.4 Chromatographic analysis of potential chromophores in the visible**

In addition to examining the integrated spectrum, we can also focus on potential chromophores that absorb in the 500 – 570 nm region of the spectrum. Considering that flaming-dominated combustion shows little in the way

of absorbing species and the abundance of these species decreases upon aging, only fresh emissions from combustion at 500 °C will be examined. Figure 6 shows the extracted wavelength chromatogram for the 500 – 510 nm region, where absorption would be most intense over this range, for Eucalyptus and Acacia combusted at 500 °C. This chromatogram has been background subtracted by the filter blank and, given that the amount of aerosol deposited on these filters was not measured, no scaling was applied. Remarkably, only a few peaks dominate the chromatogram, though there are likely several low abundance and indistinct peaks 11 – 13 minutes. The UV/visible absorption spectra for each designated peak in Figure 6 are given in Figure S4. As can be seen in Figure 6, several of these species have similar retention times. A comparison was made between these peaks, with respect to elution time. Peak A and H, despite coming from different fuels, show similar retention times and UV spectra, as can be seen in Figure S5. The same can be said for peaks B, C, I, and J, which have well separated peaks at ~340 and ~485 nm with a gradual decrease to 600 nm. Peaks D, E, and K also have the same general appearance, and may be related to B, C, I and J, but are somewhat broader and peak at slightly shorter wavelengths (332 and ~480 nm).

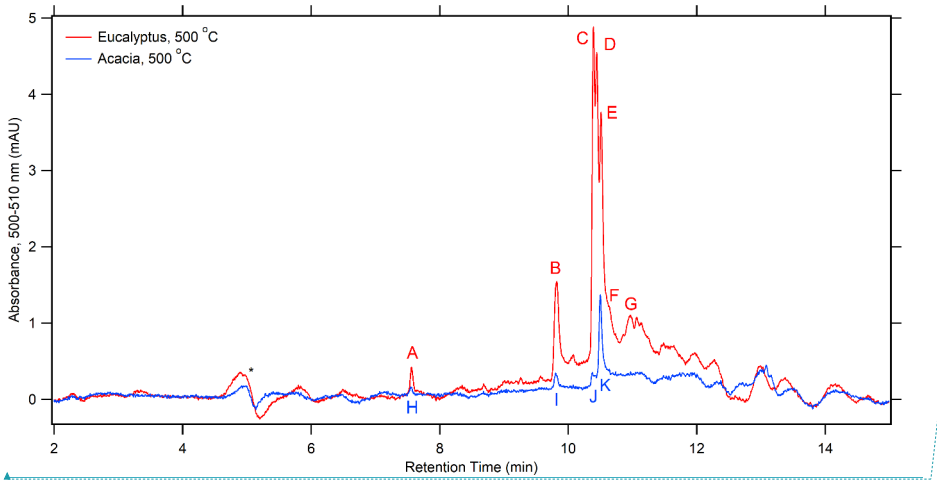

Figure 6. The extracted wavelength chromatogram for the 500 – 510 nm region for each fuel freshly combusted at 500 °C. The peak with the asterisk is an artifact from background subtraction.

To determine which species produced the absorption features shown in Figure 6, mass spectra at the absorption maxima were examined and assessed based on the peak height in the mass spectra, how well the retention times of extracted ion chromatograms matched the extracted visible wavelength chromatogram, and if a compound can be reasonably thought to absorb in the 500-510 nm region. Assignments using this method are tenuous, given that species detected by the DAD may not be seen by negative-mode ESI-MS. Additionally, many of the species described below have additional peaks outside those described, suggesting that not all isomers corresponding to a given formula absorb in this region. The extracted ion and visible chromatograms (shown in Figure 6) are in Figure S6a for

Formatted: Font:10 pt

Eucalyptus. Peak A is either $C_9H_{10}O_3$ (*m/z* 165.0559), tentatively assigned earlier, and/or $C_9H_{12}O_4$ (*m/z* 183.0658), which could be an isomer of trimethoxyphenol or dimethoxy methyl catechol. Several isomers of $C_9H_{10}O_3$ are known to only absorb below 240 nm, though veratraldehyde and caffeyl alcohol UV/visible spectra have not been measured, nor has trimethoxyphenol or dimethoxy methyl catechol for $C_9H_{12}O_4$. A $C_9H_{10}O_3$ isomer may also contribute to peak B and, while $C_8H_{10}O_2$ (*m/z* 137.0612) is more abundant at peak B and previously identified as several isomers in this work, none would absorb in this region. Likewise, $C_{10}H_{10}O_2$ (*m/z* 161.0604) elutes with peak B, which may be methoxycinnamaldehyde, methylcinnamic acid, or methylhydrocoumarin. While the spectra of those compounds have not been previously measured, it is unlikely that they would absorb in this region either. One compound that could weakly absorb in the visible and elutes at peak B is hydroxycoumarin ($C_9H_6O_3$, *m/z* 161.0244). One such compound, umbelliferone, absorbs to ~420 nm (Abu-Eittah and El-Tawil, 1985), though a number of isomers are present which may have somewhat different spectra.

Several species show peaks in the mass chromatogram that correspond to peaks B-F, including $C_{10}H_8O_3$ (*m/z* 175.0405), $C_{11}H_8O_3$ (*m/z* 187.0401), and $C_{11}H_{10}O_3$ (*m/z* 189.0565). The species corresponding to $C_{10}H_8O_3$ could be methoxycoumarin or methylhydroxycoumarin, though these species mainly absorb below ~450 nm (Abu-Eittah and El-Tawil, 1985) and may only absorb very weakly above 500 nm if at all. Naphthalenetriol is a much more likely candidate for $C_{10}H_8O_3$, given its extended and functionalized aromatic system, though a spectrum for any of its isomers has not been measured. The less functionalized 1,4-naphthalenediol absorbs to ~680 nm (Linstrom and Mallard, 2020). The structures attributable to $C_{11}H_8O_3$ could be hydroxynaphthoic acid, acetylcoumarin, or methylcoumarinaldehyde, but none of these compounds absorb above 410 nm (Donovalová et al., 2012). Still, several of these compounds are yellow solids in their pure forms according to their SDS sheets, suggesting they have some interaction with visible light. Similarly, an indistinct number of peaks associated with $C_{11}H_{10}O_3$ are found within these retention times, which may be isomers of methylmethoxycoumarin or dimethylhydroxycoumarin; none of which have previously measured spectra. Peaks in the vicinity of if peaks F and G correspond to $C_{12}H_{10}O_3$ (*m/z* 201.0554) methoxynaphthoic acid or methoxyhydroxynaphthaldehyde. No UV/visible spectra are available for these compound and, while some spectra are available for related compounds such as 1- and 2-naphthoic acid (Linstrom and Mallard, 2020), these spectra seem truncated at ~350 nm. More telling is the SDS descriptions for these substituted naphthaldehydes and naphthoic acids, which are light yellow, yellow, and light brown. This suggest that their absorption extends into the visible and possibly into the 500 nm region.

One set of isomers in the vicinity of peaks C through F correspond to the formula of $C_{11}H_6O_3$ (*m/z* 185.0256). Given the high degree of unsaturation (DBE = 9), these can only be furanocoumarins, which have a fused furan and benzene ring. Two common isomers of these species are psoralen and angelicin. While these species do not absorb in this region of this visible, they are strong absorbers below 370 nm (Rutan et al., 2018) and have not been previously identified as BrC species in BB aerosol. The peaks for nitroguaiacol/methylnitrocatechol, discussed earlier in this work, do not align well with peaks in Figure 6.

Fresh Acacia combusted at 500 °C underwent a similar analysis, as shown in Figure S6b. All of the previously mentioned extracted ion chromatograms appear very similar for Acacia, with the main difference being that the ion

abundance for Acacia was smaller by a factor or 2-4. Most ions had similar temporal profiles as Eucalyptus with the exception of $C_{11}H_{10}O_3$ (*m/z* 189.0565), which only matched peak K and onwards. Given this, it is very likely that peaks with similar DAD retention times are produced by the same species, and peak A corresponds with peak H, B with I, C with J, and E with K.

4 Conclusions

When both fuels in this work were efficiently combusted at 800 °C, the chemical characterization of fresh BB aerosol revealed very little apparent difference between the two species – Eucalyptus and Acacia. The higher SSA observed for Eucalyptus was not attributed to it containing more low abundance species, but some set of compounds that were not being captured in this analysis. This could be due to a prevalence of low abundance species, semi-volatile compounds lost during sample processing (Chen et al., 2017), or would be insensitive to ionization in the negative ion mode of our UPLC/DAD-ESI-HR-QTOFMS technique. A compound such as eucalyptol, which does not absorb in the UV or visible, could significantly alter the real portion of the refractive index of aerosols, but would not be apparent using negative ion mode ESI-MS, given its lack of basic functionality.

Comparing these species combusted at 500 °C revealed many species, differentiated by their mass and chromatographic retention time (i.e. different isomers possessing the same formula). This work focused on compounds that were significantly different between fuel types, which had scaled intensity differences greater than 0.5%. Both samples had a variety of compounds in common, such as lignin pyrolysis products, distillation products, and cellulose breakdown products. Only one isomer of dihydroxybenzene was observed for both fuels, which is either catechol (Simoneit, 2002) or resorcinol (Yokelson et al., 2013). Several lignin pyrolysis products and distillation products are more prevalent in Eucalyptus than Acacia, while pyrolysis products of cellulose and at least one nitro-aromatic species (nitroanisole, nitrocresol, or nitrobenxyl alcohol) were more prevalent in Acacia. When both fuels and Olive were examined for their sinapaldehyde and coniferaldehyde content, it was found that coniferaldehyde was more abundant by a factor of 1.6 − 3.4, depending on the species. Given that all three are angiosperms, this observation is counter to observations made by Fleming et al. (2019), though it is worth noting that their results were in terms of absorption intensity instead of ion intensity. Given that chromophores, such as lignin pyrolysis and distillation products are more prevalent in Eucalyptus than Acacia, which has a higher abundance of non-chromophores derived from sugars and cellulose, one would assume that Eucalyptus would be more absorbing in the visible (i.e. have a lower SSA) than Acacia. Despite this analysis not capturing absolute amounts of OA, Acacia was found to have an SSA that is higher than Eucalyptus by 0.1 to 0.2, which is consistent with these observations. This suggests that Acacia has either larger absolute amounts of non-chromophore compounds or Eucalyptus has a greater quantity of chromophores whose absorptive properties extend to the 500 – 570 nm region of the visible spectrum.

In examining the effects of aging in the presence of UV light and anthropogenic VOCs, it is clear from Figures 2 (Eucalyptus) and 3 (Acacia) that the amount of BrC decreases as the sample ages for combustion at 500 °C, and very few changes are occurring for particles produced from combustion at 800 °C. For both Eucalyptus and Acacia, an isomer of dihydroxybenzene, such as resorcinol or catechol, was removed to the highest degree from the

Deleted:

fresh BB aerosol. Both of these species have relatively broad UV absorption spectra, extending from the vacuum UV to ~292 nm, with a peak at 275 nm and another at shorter wavelengths (Dewar et al., 1958). This is where most of the reduction of UV absorption is occurring. While this could suggest that these two compounds are responsible for a significant portion of the bleaching effect, there are a great number of compounds that absorb in a similar wavelength range, so that could not be conclusively stated. The removal of dihydroxybenzene was investigated by examining spectra for a known reaction product, dihydroxynitrobenzene (e.g. nitrocatechol). Results for both fuels suggest a small amount was produced by primary emissions, but it was mainly a product of secondary formation. The second most removed compound for Eucalyptus was the distillation product benzoic acid and the lignin pyrolysis product hydroxybenzaldehyde. Several Eucalyptus distillation products are also sensitive to aging that have not been previously observed, such as seven isomers of methoxy- and/or methylhydroxycoumarin and all 6 isomers of hydroxycoumarin, of which only one has been previously observed. The second most consumed compound for Acacia was one isomer that is likely nitroanisole, nitrobenxyl alcohol, or nitrocresol, which was not seen previously and is a primary product of in-flame NO_x chemistry. Generally, both fuels were dominated by loss of chromatophoric lignin pyrolysis and distillation products. Focusing on nitroaromatic species, one isomer of nitrophenol was produced during the aging of Acacia combusted at 500 °C, while none was produced for Eucalyptus. Despite being thought of as a tracer for BB SOA (Iinuma et al., 2010), there is evidence for both primary emission and secondary production of 4-methyl-5-nitrocatechol.

Deleted: /or

Deleted:

Not surprisingly, the associated absorbance from these chromophores, mostly from 200 – 350 nm, also attenuates with respect to age, as seen in Figure 5. This may be caused in part by the photo-bleaching effect created by irradiation of UV light for 12 hours, heterogeneous OH oxidation, and SOA formation of non-chromophores. As stated in Part I of this companion paper, ignition temperature is the leading factor for differences in the SSA of the resulting BB aerosol, which is supported by the associated MCE values at each temperature. At lower temperatures, combustion is less efficient and releases more emissions in the form of the lignin pyrolysis and distillation products, which are primarily responsible for the change in absorption seen between fresh and aged samples, as they absorb strongly in the UV. Some larger compounds were discovered, but only one functionalized PAH was successfully identified. The identification of other functionalized PAHs would be beneficial in determining any changes to SSA because of photochemical aging with anthropogenic VOCs present, as these compounds exhibit wide absorption spectra extending into the visible.

An attempt was also made to identify which species produce absorption at wavelengths longer than 500 nm. An extracted wavelength chromatogram from 500 – 510 nm shows only a few peaks dominate the absorption from fresh emissions of combustion at 500 °C. Both Acacia and Eucalyptus have common absorbing species, as shown by peaks with common retention times, similar UV/Visible spectra, and extracted ion chromatograms. By comparing the retention times of extracted ion and wavelength chromatograms, several species were tentatively suggested for contributing to absorption in this wavelength range. This includes functionalized courmarin species (hydroxy-, methoxy- methylhydroxy-, methylmethoxy-, etc.), naphthalenetriol, and methoxyhydroxynaphthaldehyde or methoxynaphthoic acid. UV spectra available from the literature for several of these species and/or related compounds seem truncated and are very likely to extend into this visible region of the spectrum, which highlights the need for

broadband UV/Visible spectral measurements of these compounds. While not important for absorption in this visible region, a novel set of compounds were found that could be strong BrC species – furanocoumarins.

As shown in companion paper Part 1, there are changes in the SSA that occur in response to dark aging. Future work will examine those processes from a molecular standpoint, and how they are different from photochemical aging. Given that there was no SOA enhancement or significant difference in SSA observed for the addition of anthropogenic VOCs, it is unlikely that even these elevated concentrations would alter the molecular constituents either. However, this should be confirmed with at least one example.

Author contribution: Damon Smith and Tianqu Cui conducted the experiments, Marc Fiddler, Tianqu Cui, and Damon Smith analyzed the data. Marc Fiddler, Jason Surratt and Solomon Bililign designed the experiments and contributed to writing and editing. Rudra Pokhrel contributed to the data analysis and interpretation.

Deleted: and analyzed the data

Competing interests: The authors declare that they have no conflict of interest.

References

Abu-Eittah, R. H., and El-Tawil, B. A. H.: The electronic absorption spectra of some coumarins. A molecular orbital treatment, Canadian Journal of Chemistry, 63, 1173-1179, 10.1139/v85-200, 1985.

Akagi, S. K., Yokelson, R. J., Wiedinmyer, C., Alvarado, M. J., Reid, J. S., Karl, T., Crounse, J. D., and Wennberg, P. O.: Emission factors for open and domestic biomass burning for use in atmospheric models, Atmos. Chem. Phys., 11, 4039-4072, 10.5194/acp-11-4039-2011, 2011.

Andreae, M. O., and Merlet, P.: Emission of trace gases and aerosols from biomass burning, Global Biogeochemical Cycles, 15, 955-966, 10.1029/2000GB001382, 2001.

Andreae, M. O., and Gelencsér, A.: Black carbon or brown carbon? The nature of light-absorbing carbonaceous aerosols, Atmos. Chem. Phys., 6, 3131-3148, 10.5194/acp-6-3131-2006, 2006.

Bergstrom, R. W., Pilewskie, P., Russell, P. B., Redemann, J., Bond, T. C., Quinn, P. K., and Sierau, B.: Spectral absorption properties of atmospheric aerosols, Atmos. Chem. Phys., 7, 5937-5943, 10.5194/acp-7-5937-2007, 2007.

Bi, X., Simoneit, B. R. T., Sheng, G., Ma, S., and Fu, J.: Composition and major sources of organic compounds in urban aerosols, Atmospheric Research, 88, 256-265, https://doi.org/10.1016/j.atmosres.2007.11.017, 2008.

Bluvshtein, N., Lin, P., Flores, J. M., Segev, L., Mazar, Y., Tas, E., Snider, G., Weagle, C., Brown, S. S., Laskin, A., and Rudich, Y.: Broadband optical properties of biomass-burning aerosol and identification of brown carbon chromophores, J. Geophys. Res.: Atmos., 122, 5441-5456, 10.1002/2016JD026230, 2017.

Bond, T. C., and Bergstrom, R. W.: Light Absorption by Carbonaceous Particles: An Investigative Review, Aerosol Science and Technology, 40, 27-67, 10.1080/02786820500421521, 2006.

Budisulistiorini, S. H., Riva, M., Williams, M., Chen, J., Itoh, M., Surratt, J. D., and Kuwata, M.: Light-Absorbing Brown Carbon Aerosol Constituents from Combustion of Indonesian Peat and Biomass, Environmental Science & Technology, 51, 4415-4423, 10.1021/acs.est.7b00397, 2017.

Chen, J., Li, C., Ristovski, Z., Milic, A., Gu, Y., Islam, M. S., Wang, S., Hao, J., Zhang, H., He, C., Guo, H., Fu, H., Miljevic, B., Morawska, L., Thai, P., Lam, Y. F., Pereira, G., Ding, A., Huang, X., and Dumka, U. C.: A review of biomass burning: Emissions and impacts on air quality, health and climate in China, Science of The Total Environment, 579, 1000-1034, https://doi.org/10.1016/j.scitotenv.2016.11.025, 2017.

Chen, Y., and Bond, T. C.: Light absorption by organic carbon from wood combustion, Atmos. Chem. Phys., 10, 1773-1787, 10.5194/acp-10-1773-2010, 2010.

Collier, S., Zhou, S., Onasch, T. B., Jaffe, D. A., Kleinman, L., Sedlacek, A. J., Briggs, N. L., Hee, J., Fortner, E., and Shilling, J. E.: Regional Influence of Aerosol Emissions from Wildfires Driven by Combustion Efficiency: Insights from the BBOP Campaign, Environ. Sci. Technol., 50, 8613, 2016.

Dasari, S., Andersson, A., Bikkina, S., Holmstrand, H., Budhavant, K., Satheesh, S., Asmi, E., Kesti, J., Backman, J., Salam, A., Bisht, D. S., Tiwari, S., Hameed, Z., and Gustafsson, Ö.: Photochemical degradation affects the light absorption of water-soluble brown carbon in the South Asian outflow, Science Advances, 5, eaau8066, 10.1126/sciadv.aau8066, 2019.

Dewar, M. J. S., Kubba, V. P., and Pettit, R.: 625. New heteroaromatic compounds. Part II. Boron compounds isoconjugate with indole, 2 : 3-benzofuran, and thionaphthen, Journal of the Chemical Society (Resumed), 3076-3079, 10.1039/JR9580003076, 1958.
Donovalová, J., Cigáň, M., Stankovičová, H., Gašpar, J., Danko, M., Gáplovský, A., and Hrdlovič, P.: Spectral Properties of Substituted Coumarins in Solution and Polymer Matrices, Molecules, 17, 3259-3276, 10.3390/molecules17033259, 2012.
Finewax, Z., de Gouw, J. A., and Ziemann, P. J.: Identification and Quantification of 4-Nitrocatechol Formed from OH and NO3 Radical-Initiated Reactions of Catechol in Air in the Presence of NOx: Implications for Secondary Organic Aerosol Formation from Biomass Burning, Environ. Sci. Technol., 52, 1981-1989, 10.1021/acs.est.7b05864, 2018.
Fleming, L. T., Lin, P., Roberts, J. M., Selimovic, V., Yokelson, R., Laskin, J., Laskin, A., and Nizkorodov, S. A.: Molecular composition and photochemical lifetimes of brown carbon chromophores in biomass burning organic aerosol, Atmos. Chem. Phys. Discuss., 2019, 1-38, 10.5194/acp-2019-523, 2019.
Fortner, E., Onasch, T., Canagaratna, M., Williams, L. R., Lee, T., Jayne, J., and Worsnop, D.: Examining the chemical composition of black carbon particles from biomass burning with SP-AMS, Journal of Aerosol Science, 120, 12-21, https://doi.org/10.1016/j.jaerosci.2018.03.001, 2018.
Iinuma, Y., Böge, O., Gräfe, R., and Herrmann, H.: Methyl-Nitrocatechols: Atmospheric Tracer Compounds for Biomass Burning Secondary Organic Aerosols, Environmental Science & Technology, 44, 8453-8459, 10.1021/es102938a, 2010.
Jiang, H., Frie, A. L., Lavi, A., Chen, J. Y., Zhang, H., Bahreini, R., and Lin, Y.-H.: Brown Carbon Formation from Nighttime Chemistry of Unsaturated Heterocyclic Volatile Organic Compounds, Environmental Science & Technology Letters, 6, 184-190, 10.1021/acs.estlett.9b00017, 2019.
Kirchstetter, T. W., Novakov, T., and Hobbs, P. V.: Evidence that the spectral dependence of light absorption by aerosols is affected by organic carbon, Journal of Geophysical Research: Atmospheres, 109, doi:10.1029/2004JD004999, 2004.
Kitanovski, Z., Grgić, I., Vermeylen, R., Claeys, M., and Maenhaut, W.: Liquid chromatography tandem mass spectrometry method for characterization of monoaromatic nitro-compounds in atmospheric particulate matter, Journal of Chromatography A, 1268, 35-43, https://doi.org/10.1016/j.chroma.2012.10.021, 2012a.
Kitanovski, Z., Grgić, I., Yasmeen, F., Claeys, M., and Čusak, A.: Development of a liquid chromatographic method based on ultraviolet–visible and electrospray ionization mass spectrometric detection for the identification of nitrocatechols and related tracers in biomass burning atmospheric organic aerosol, Rapid Communications in Mass Spectrometry, 26, 793-804, 10.1002/rcm.6170, 2012b.
Kroflič, A., Huš, M., Grilc, M., and Grgić, I.: Underappreciated and Complex Role of Nitrous Acid in Aromatic Nitration under Mild Environmental Conditions: The Case of Activated Methoxyphenols, Environmental Science & Technology, 52, 13756-13765, 10.1021/acs.est.8b01903, 2018.
Kumar, N. K., Corbin, J. C., Bruns, E. A., Massabó, D., Slowik, J. G., Drinovec, L., Močnik, G., Prati, P., Vlachou, A., Baltensperger, U., Gysel, M., El-Haddad, I., and Prévôt, A. S. H.: Production of particulate brown carbon during atmospheric aging of residential wood-burning emissions, Atmospheric Chemistry and Physics, 18, 17843-17861, 10.5194/acp-18-17843-2018, 2018.

Lambe, A. T., Ahern, A. T., Williams, L. R., Slowik, J. G., Wong, J. P. S., Abbatt, J. P. D., Brune, W. H., Ng, N. L., Wright, J. P., and Croasdale, D. R.: Characterization of Aerosol Photooxidation Flow Reactors: Heterogeneous Oxidation, Secondary Organic Aerosol Formation and Cloud Condensation Nuclei Activity Measurements, Atmos. Meas. Tech., 4, 445, 2011.

Lambe, A. T., Cappa, C. D., Massoli, P., Onasch, T. B., Forestieri, S. D., Martin, A. T., Cummings, M. J., Croasdale, D. R., Brune, W. H., Worsnop, D. R., and Davidovits, P.: Relationship between Oxidation Level and Optical Properties of Secondary Organic Aerosol, Environmental Science & Technology, 47, 6349-6357, 10.1021/es401043j, 2013.

Laskin, A., Laskin, J., and Nizkorodov, S. A.: Chemistry of Atmospheric Brown Carbon, Chemical Reviews, 115, 4335-4382, 10.1021/cr5006167, 2015.

Laskin, A., Lin, P., Laskin, J., Fleming, L., and Nizkorodov, S.: Molecular Characterization of Atmospheric Brown Carbon, in: Multiphase Environmental Chemistry in the Atmosphere, edited by: Hunt, S. W., Laskin, A., and Nizkorodov, S. A., American Chemical Society, 261-274, 2018.

Lee, H. J., Aiona, P. K., Laskin, A., Laskin, J., and Nizkorodov, S. A.: Effect of Solar Radiation on the Optical Properties and Molecular Composition of Laboratory Proxies of Atmospheric Brown Carbon, Environmental Science & Technology, 48, 10217-10226, 10.1021/es502515r, 2014.

Lin, P., Laskin, J., Nizkorodov, S. A., and Laskin, A.: Revealing Brown Carbon Chromophores Produced in Reactions of Methylglyoxal with Ammonium Sulfate, Environmental Science & Technology, 49, 14257-14266, 10.1021/acs.est.5b03608, 2015a.

Lin, P., Liu, J. M., Shilling, J. E., Kathmann, S. M., Laskin, J., and Laskin, A.: Molecular characterization of brown carbon (BrC) chromophores in secondary organic aerosol generated from photo-oxidation of toluene, Phys. Chem. Chem. Phys., 17, 23312, 2015b.

Lin, P., Aiona, P. K., Li, Y., Shiraiwa, M., Laskin, J., Nizkorodov, S. A., and Laskin, A.: Molecular Characterization of Brown Carbon in Biomass Burning Aerosol Particles, Environmental Science & Technology, 50, 11815-11824, 10.1021/acs.est.6b03024, 2016.

Lin, P., Bluvshtein, N., Rudich, Y., Nizkorodov, S. A., Laskin, J., and Laskin, A.: Molecular Chemistry of Atmospheric Brown Carbon Inferred from a Nationwide Biomass Burning Event, Environmental Science & Technology, 51, 11561-11570, 10.1021/acs.est.7b02276, 2017.

Lin, Y.-H., Budisulistiorini, S. H., Chu, K., Siejack, R. A., Zhang, H., Riva, M., Zhang, Z., Gold, A., Kautzman, K. E., and Surratt, J. D.: Light-Absorbing Oligomer Formation in Secondary Organic Aerosol from Reactive Uptake of Isoprene Epoxydiols, Environmental Science & Technology, 48, 12012-12021, 10.1021/es503142b, 2014.

NIST Chemistry WebBook, NIST Standard Reference Database Number 69, access: August 1, 2020.

Liu, D., Whitehead, J., Alfarra, M. R., Reyes-Villegas, E., Spracklen, Dominick V., Reddington, Carly L., Kong, S., Williams, Paul I., Ting, Y.-C., Haslett, S., Taylor, Jonathan W., Flynn, Michael J., Morgan, William T., McFiggans, G., Coe, H., and Allan, James D.: Black-carbon absorption enhancement in the atmosphere determined by particle mixing state, Nature Geoscience, 10, 184, 10.1038/ngeo2901 https://www.nature.com/articles/ngeo2901 - supplementary-information, 2017.

Masamba, W. R. L., Henry, E. M. T., and Banda, W.: Composition and properties of essential oils from Eucalyptus camaldulensis and E. tereticornis, Malawi J. Sci. Technol., 6, 81-89, 2001.

May, A. A., McMeeking, G. R., Lee, T., Taylor, J. W., Craven, J. S., Burling, I., Sullivan, A. P., Akagi, S., Collett Jr., J. L., Flynn, M., Coe, H., Urbanski, S. P., Seinfeld, J. H., Yokelson, R. J., and Kreidenweis, S. M.: Aerosol emissions from prescribed fires in the United States: A

synthesis of laboratory and aircraft measurements, Journal of Geophysical Research: Atmospheres, 119, 11,826-811,849, 10.1002/2014jd021848, 2014.
McClure, C. D., Lim, C. Y., Hagan, D. H., Kroll, J. H., and Cappa, C. D.: Biomass-burning derived particles from a wide variety of fuels: Part 1: Properties of primary particles, Atmos. Chem. Phys. Discuss., 2019, 1-37, 10.5194/acp-2019-707, 2019.
McMeeking, G. R., Kreidenweis, S. M., Baker, S., Carrico, C. M., Chow, J. C., Collett, J. L., Hao, W. M., Holden, A. S., Kirchstetter, T. W., Malm, W. C., Moosmüller, H., Sullivan, A. P., and Wold, C. E.: Emissions of trace gases and aerosols during the open combustion of biomass in the laboratory, Journal of Geophysical Research: Atmospheres, 114, D19210, 10.1029/2009JD011836, 2009.
Mohr, C., Lopez-Hilfiker, F. D., Zotter, P., Prévôt, A. S. H., Xu, L., Ng, N. L., Herndon, S. C., Williams, L. R., Franklin, J. P., Zahniser, M. S., Worsnop, D. R., Knighton, W. B., Aiken, A. C., Gorkowski, K. J., Dubey, M. K., Allan, J. D., and Thornton, J. A.: Contribution of Nitrated Phenols to Wood Burning Brown Carbon Light Absorption in Detling, United Kingdom during Winter Time, Environmental Science & Technology, 47, 6316-6324, 10.1021/es400683v, 2013.
Moise, T., Flores, J. M., and Rudich, Y.: Optical Properties of Secondary Organic Aerosols and Their Changes by Chemical Processes, Chemical Reviews, 115, 4400-4439, 10.1021/cr5005259, 2015.
Nguyen, T. B., Lee, P. B., Updyke, K. M., Bones, D. L., Laskin, J., Laskin, A., and Nizkorodov, S. A.: Formation of nitrogen- and sulfur-containing light-absorbing compounds accelerated by evaporation of water from secondary organic aerosols, Journal of Geophysical Research: Atmospheres, 117, 10.1029/2011jd016944, 2012.
Oyem, A. A., and Igbafe, A. F.: Analysis of Atmospheric Aerosol Loading over Nigeria, Environmental Research Journal, 4, 145-156, 2010.
Qin, Y. M., Tan, H. B., Li, Y. J., Li, Z. J., Schurman, M. I., Liu, L., Wu, C., and Chan, C. K.: Chemical characteristics of brown carbon in atmospheric particles at a suburban site near Guangzhou, China, Atmos. Chem. Phys., 18, 16409-16418, 10.5194/acp-18-16409-2018, 2018.
Reid, J., Koppmann, R., Eck, T., and Eleuterio, D.: A review of biomass burning emissions part II: intensive physical properties of biomass burning particles, Atmospheric Chemistry and Physics, 5, 799-825, https://doi.org/10.5194/acp-5-799-2005, 2005.
Rutan, S. C., Venkatramani, C. J., and Stoll, D. R.: Peak Purity in Liquid Chromatography, Part I: Basic Concepts, Commercial Software, and Limitations, LCGC North America, 36, 100-110, 2018.
Saleh, R., Hennigan, C. J., McMeeking, G. R., Chuang, W. K., Robinson, E. S., Coe, H., Donahue, N. M., and Robinson, A. L.: Absorptivity of brown carbon in fresh and photo-chemically aged biomass-burning emissions, Atmos. Chem. Phys., 13, 7683-7693, 10.5194/acp-13-7683-2013, 2013.
Saleh, R., Cheng, Z., and Atwi, K.: The Brown–Black Continuum of Light-Absorbing Combustion Aerosols, Environmental Science & Technology Letters, 5, 508-513, 10.1021/acs.estlett.8b00305, 2018.
Saleh, R.: From Measurements to Models: Toward Accurate Representation of Brown Carbon in Climate Calculations, Current Pollution Reports, 6, 90-104, 10.1007/s40726-020-00139-3, 2020.
Sareen, N., Moussa, S. G., and McNeill, V. F.: Photochemical Aging of Light-Absorbing Secondary Organic Aerosol Material, The Journal of Physical Chemistry A, 117, 2987-2996, 10.1021/jp309413j, 2013.

Schnitzler, E. G., and Abbatt, J. P. D.: Heterogeneous OH oxidation of secondary brown carbon aerosol, Atmos. Chem. Phys., 18, 14539-14553, 10.5194/acp-18-14539-2018, 2018.
Schuster, G. L., Dubovik, O., Arola, A., Eck, T. F., and Holben, B. N.: Remote sensing of soot carbon – Part 2: Understanding the absorption Ångström exponent, Atmos. Chem. Phys., 16, 1587-1602, 10.5194/acp-16-1587-2016, 2016.
Simoneit, B. R. T.: Biomass burning — a review of organic tracers for smoke from incomplete combustion, Applied Geochemistry, 17, 129-162, https://doi.org/10.1016/S0883-2927(01)00061-0, 2002.
Simoneit, B. R. T., Elias, V. O., Kobayashi, M., Kawamura, K., Rushdi, A. I., Medeiros, P. M., Rogge, W. F., and Didyk, B. M.: Sugars - Dominant water-soluble organic compounds in soils and characterization as tracers in atmospheric particulate matter, Environmental Science & Technology, 38, 5939-5949, 10.1021/es0403099, 2004.
Smith, D. M., Fiddler, M. N., Sexton, K. G., and Bililign, S.: Construction and Characterization of an Indoor Smog Chamber for Measuring the Optical and Physicochemical Properties of Aging Biomass Burning Aerosols, Aerosol and Air Quality Research, 19, 467-483, 10.4209/aaqr.2018.06.0243, 2019.
Smith, D. M., Fiddler, M. N., Pokhrel, R., and Bililign, S.: Laboratory studies of fresh and aged biomass burning aerosols emitted from east African biomass fuels – Part 1 – Optical properties, Atmos. Chem. Phys. Discuss., 2020, 1-30, 10.5194/acp-2019-1156, 2020.
Subramanian, P. A., Gebrekidan, A., and Nigussie, K.: Yield, contents and chemical composition variations in the essential oils of different Eucalyptus globulus trees from Tigray, Northern Ethiopia, J. Pharm. Biomed. Sci., 11, 2012.
Sumlin, B. J., Pandey, A., Walker, M. J., Pattison, R. S., Williams, B. J., and Chakrabarty, R. K.: Atmospheric Photooxidation Diminishes Light Absorption by Primary Brown Carbon Aerosol from Biomass Burning, Environmental Science & Technology Letters, 4, 540-545, 10.1021/acs.estlett.7b00393, 2017.
Tautenhahn, R., Patti, G. J., Rinehart, D., and Siuzdak, G.: XCMS Online: A Web-Based Platform to Process Untargeted Metabolomic Data, Analytical Chemistry, 84, 5035-5039, 10.1021/ac300698c, 2012.
Teich, M., van Pinxteren, D., Wang, M., Kecorius, S., Wang, Z., Müller, T., Močnik, G., and Herrmann, H.: Contributions of nitrated aromatic compounds to the light absorption of water-soluble and particulate brown carbon in different atmospheric environments in Germany and China, Atmos. Chem. Phys., 17, 1653-1672, 10.5194/acp-17-1653-2017, 2017.
Tian, Z., Gold, A., Nakamura, J., Zhang, Z., Vila, J., Singleton, D. R., Collins, L. B., and Aitken, M. D.: Nontarget Analysis Reveals a Bacterial Metabolite of Pyrene Implicated in the Genotoxicity of Contaminated Soil after Bioremediation, Environmental Science & Technology, 51, 7091-7100, 10.1021/acs.est.7b01172, 2017.
Tichy, M.: UV Atlas of Organic Compounds, in: UV Atlas of Organic Compounds / UV Atlas organischer Verbindungen, Springer US, Boston, MA, 5-605, 1967.
Vidovic, K., Lasic Jurkovic, D., Sala, M., Kroflic, A., and Grgic, I.: Nighttime Aqueous-Phase Formation of Nitrocatechols in the Atmospheric Condensed Phase, Environ. Sci. Technol., 52, 9722-9730, 10.1021/acs.est.8b01161, 2018.
Wang, Y., Hu, M., Wang, Y., Zheng, J., Shang, D., Yang, Y., Liu, Y., Li, X., Tang, R., Zhu, W., Du, Z., Wu, Y., Guo, S., Wu, Z., Lou, S., Hallquist, M., and Yu, J. Z.: The formation of nitro-aromatic compounds under high NOx and anthropogenic VOC conditions in urban Beijing, China, Atmos. Chem. Phys., 19, 7649-7665, 10.5194/acp-19-7649-2019, 2019.

Yokelson, R. J., Burling, I. R., Gilman, J. B., Warneke, C., Stockwell, C. E., de Gouw, J., Akagi, S. K., Urbanski, S. P., Veres, P., Roberts, J. M., Kuster, W. C., Reardon, J., Griffith, D. W. T., Johnson, T. J., Hosseini, S., Miller, J. W., Cocker Iii, D. R., Jung, H., and Weise, D. R.: Coupling field and laboratory measurements to estimate the emission factors of identified and unidentified trace gases for prescribed fires, Atmos. Chem. Phys., 13, 89-116, 10.5194/acp-13-89-2013, 2013.

Zhang, X., Lin, Y.-H., Surratt, J. D., and Weber, R. J.: Sources, Composition and Absorption Ångström Exponent of Light-absorbing Organic Components in Aerosol Extracts from the Los Angeles Basin, Environmental Science & Technology, 47, 3685-3693, 10.1021/es305047b, 2013.

Zhao, R., Lee, A. K. Y., Huang, L., Li, X., Yang, F., and Abbatt, J. P. D.: Photochemical processing of aqueous atmospheric brown carbon, Atmos. Chem. Phys., 15, 6087-6100, 10.5194/acp-15-6087-2015, 2015.